Chapter Five

Source Localization: Subspace Methods

The location parameters are estimated directly without having to search for peaks as in frequency-wavenumber spectrum (the approach described in chapter 4). In open space the direction of arrival (DOA), that is, azimuth or elevation or both, is estimated using the subspace properties of the spatial covariance matrix or spectral matrix. MUSIC is a well known algorithm where we define a positive quantity which becomes infinity whenever the assumed parameter(s) is equal to the true parameter. We shall call this quantity as a spectrum even though it does not possess the units of power as in the true spectrum. The MUSIC algorithm in its original form does involve scanning and searching, often very fine scanning lest we may miss the peak. Later extensions of the MUSIC, like root MUSIC, ESPRIT, etc. have overcome this limitation of the original MUSIC algorithm. When a source is located in a bounded space, such as a duct, the wavefront reaching an array of sensors is necessarily nonplanar due to multipath propagation in the bounded space. In this case all three position parameters can be measured by means of an array of sensors. But the complexity of the problem of localization is such that a good prior knowledge of the channel becomes mandatory for successful localization. In active systems, since one has control over the source, it is possible to design waveforms which possess the property that is best suited for localization; for example, a binary phase shift key (BPSK) signal with its narrow autocorrelation function is best suited for time delay estimation. Source tracking of a moving source is another important extension of the source localization problem.

§5.1 **Subspace Methods** (Narrowband):

Earlier we showed an interesting property of eigenvalues and eigenvectors of a spectral matrix of a wavefield which consists of uncorrelated plane waves in the presence of white noise. Specifically, equations (4.14a) and (4.14b) form the basis for the signal subspace method for DOA estimation. For convenience, those two equations are reproduced here

$$\lambda_m = \alpha_m + \sigma_\eta^2 \tag{4.14a}$$

$$\mathbf{v}_m^H \mathbf{A} = \mathbf{0}, \qquad \text{for} \qquad m = P, P+1, \ldots, M-1 \tag{4.14b}$$

Equation (4.14b) implies that the space spanned by the columns of $\mathbf{A}$, that is, the direction vectors of incident wavefronts, is orthogonal to the space spanned by the eigenvectors, $\mathbf{v}_m$, $m = P, P+1, \ldots, M-1$, often known as noise subspace, $\mathbf{v}_\eta$. The space spanned by the columns of $\mathbf{A}$ is known as signal subspace, $\mathbf{v}_s$. Consider the space spanned by a steering vector, $\mathbf{a}(\omega,\theta)=col\left\{1,e^{-j\omega\frac{d}{c}\sin\theta},e^{-j2\omega\frac{d}{c}\sin\theta},\ldots,e^{-j(M-1)\omega\frac{d}{c}\sin\theta}\right\}$, as the steering angle is varied over a range $\pm\frac{\pi}{2}$. The intersection of the array manifold with the signal subspace yields the direction vectors of the signals.

5.1.1 MUSIC: On account of (4.14b) a steering vector pointing in the direction of one of the incident wavefronts will be orthogonal to the noise subspace,

$$\mathbf{v}_m^H\mathbf{a}(\omega,\theta)=0, \quad m=P,P+1,\ldots,M-1 \tag{5.1}$$

where $\theta=\theta_0,\theta_1,\ldots,\theta_{P-1}$. For narrowband signals the matrix $\mathbf{A}$ is given by

$$\mathbf{A}=\left[\mathbf{a}(\omega_0\frac{d}{c}\sin\theta_0),\mathbf{a}(\omega_1\frac{d}{c}\sin\theta_1),\ldots,\mathbf{a}(\omega_{P-1}\frac{d}{c}\sin\theta_{P-1})\right] \tag{5.2}$$

where we take a wavefront with a center frequency ω_p to be incident at an angle θ_p. Further, we assume that the center frequencies of the narrowband signals are known. We define a quadratic function involving a steering vector and noise subspace,

$$S_{Music}(\omega,\theta)=\frac{1}{\mathbf{a}^H(\omega,\theta)\mathbf{v}_\eta\mathbf{v}_\eta^H\mathbf{a}(\omega,\theta)} \tag{5.3}$$

$S_{Music}(\omega,\theta)$, also known as the eigenvector spectrum, will show sharp peaks whenever $\theta=\theta_0,\theta_1,\ldots,\theta_{P-1}$. The subscript *Music* stands for Multiple Signal Classification. This acronym was coined by Schmidt [1] who discovered the subspace algorithm. At about the same time but independently Bienvenu and Kopp [2] proposed a similar algorithm. Pisarenko [3] had previously published a subspace based algorithm in the context of harmonic analysis of time series. Note that, although we refer to $S_{Music}(\omega,\theta)$ as spectrum, it does not have the units of power; hence it is not a true spectrum. Let us express the steering vector in terms of the product of frequency and time delay $\tau=\frac{d}{c}\sin\theta$,

$$\mathbf{a}(\omega\tau)=col\left\{1,e^{j\omega\tau},e^{j2\omega\tau},\ldots,e^{j(M-1)\omega\tau}\right\}$$

The peaks of $S_{Music}(\omega,\theta)$ will now be at $\omega\tau = \omega_0\tau_0, \omega_1\tau_1, \ldots, \omega_{P-1}\tau_{P-1}$ and given the frequencies we can estimate the delays but there is one difficulty. It is possible that two wavefronts with different center frequencies may arrive at such angles that $\omega_p \frac{d}{c}\sin\theta_p = \omega_{p'}\frac{d}{c}\sin\theta_{p'}$, in which case the two direction vectors will become identical, causing a loss of the full column rank property of the matrix $\mathbf{A}$. When the frequencies are unknown, evidently, the delays or DOA's cannot be uniquely estimated.

We now turn to the signal subspace spanned by the eigenvectors corresponding to eigenvalues $\lambda_m = \alpha_m + \sigma_\eta^2, \quad m = 0,1,\ldots,P-1$. We shall show that the signal subspace is the same as the space spanned by the columns of the matrix $\mathbf{A}$. Since $\mathbf{A}$ is a full rank matrix its polar decomposition gives

$$\mathbf{A} = \mathbf{TG} \tag{5.4}$$

where $\mathbf{G}$ is a full rank PxP matrix and $\mathbf{T}$ is a MxP matrix satisfying the following property,

$$\mathbf{T}^H\mathbf{T} = \mathbf{I} \qquad \text{(PxP unit matrix)}$$

In (4.14a) we shall replace $\mathbf{A}$ by its polar decomposition (5.4)

$$\mathbf{v}_m^H \mathbf{A}\mathbf{C}_0\mathbf{A}^H\mathbf{v}_m = \alpha_m \tag{5.5a}$$

or in matrix form

$$\mathbf{v}_s^H \mathbf{T}\left[\mathbf{G}\mathbf{C}_0\mathbf{G}^H\right]\mathbf{T}^H\mathbf{v}_s = diag\left\{\alpha_m, m = 0,1,\ldots,P-1\right\} \tag{5.5b}$$

Let $\mathbf{T} = \mathbf{v}_s$, which is consistent with the assumed properties of $\mathbf{T}$. Equation (5.5b) now reduces to

$$\mathbf{G}\mathbf{C}_0\mathbf{G}^H = diag\left\{\alpha_m, m = 0,1,\ldots,P-1\right\} \tag{5.6a}$$

and

$$\mathbf{A} = \mathbf{v}_s\mathbf{G} \tag{5.6b}$$

We can estimate $\mathbf{G}$ from (5.6b) by premultiplying both sides by $\mathbf{v}_s^H$ and obtain

$$\mathbf{G} = \mathbf{v}_s^H \mathbf{A} \tag{5.6c}$$

Thus, the space spanned by $\mathbf{A}$ and $\mathbf{v}_s^H$ are identical. Further, by eliminating $\mathbf{G}$ from (5.6b) and (5.6c) we obtain an interesting result

$$\mathbf{A} = \mathbf{v}_s \mathbf{v}_s^H \mathbf{A} \tag{5.6d}$$

Let us define a complementary orthogonal space $(\mathbf{I} - \mathbf{v}_s \mathbf{v}_s^H)$ which will also be orthogonal to $\mathbf{A}$; therefore, $\mathbf{A}^H (\mathbf{I} - \mathbf{v}_s \mathbf{v}_s^H) \mathbf{A} = 0$. An equivalent definition of Music spectrum may be given using $(\mathbf{I} - \mathbf{v}_s \mathbf{v}_s^H)$,

$$S_{Music}(\omega, \theta) = \frac{1}{\mathbf{a}^H(\omega, \theta)(\mathbf{I} - \mathbf{v}_s \mathbf{v}_s^H)\mathbf{a}(\omega, \theta)} \tag{5.7}$$

<u>Signal Eigenvalues and Source Power</u>: The signal eigenvalues and source power are related, although the relationship is rather involved except for the single source case. Let us first consider a single source case. The covariance matrix is given by $\mathbf{C}_0 = \mathbf{a}_0 s_0 \mathbf{a}_0^H$ which we use in (5.5a) and obtain

$$s_0 = \frac{\alpha_0}{\left| \mathbf{v}_0^H \mathbf{a}_0 \right|^2} \tag{5.8}$$

Since $\mathbf{v}_0$ and $\mathbf{a}_0$ span the same space, $\mathbf{v}_0 = g_0 \mathbf{a}_0$ where g_0 is a constant which may be obtained by requiring that $\mathbf{v}_0^H \mathbf{v}_0 = 1$. We obtain $g_0 = \frac{1}{\sqrt{M}}$. Equation (5.8) reduces to $s_0 = \frac{\alpha_0}{M}$. Next we consider the two-source case. The covariance function is given by

$$\mathbf{C}_f = [\mathbf{a}_0, \mathbf{a}_1] \begin{bmatrix} s_0 & 0 \\ 0 & s_1 \end{bmatrix} [\mathbf{a}_0, \mathbf{a}_1]^H$$

and using (5.5a) we obtain

$$\mathbf{v}_s^H \mathbf{A} \mathbf{C}_0 \mathbf{A}^H \mathbf{v}_s = diag\{\alpha_0, \alpha_1\} \tag{5.9a}$$

azimuths	power #1 source	power #2 source
30^o, 40^o	1.00	1.00
30^o, 35^o	1.00	1.00
30^o, 33^o	1.00	1.00
30^o, 31^o	1.00	1.00
30^o, 30.5^o	1.00	1.00

Table 5.1 Estimation of power given the azimuths of two equal power wavefronts incident on a 16 sensor ULA. Power estimates are error-free even when the wavefronts are closely spaced.

$$\mathbf{C}_0 = \left[\mathbf{v}_s^H \mathbf{A}\right]^{-1} diag\{\alpha_0, \alpha_1\}\left[\mathbf{A}^H \mathbf{v}_s\right]^{-1} \tag{5.9b}$$

Equation (5.9b) has been used to estimate the powers of two equal power (snr=1.0) wavefronts incident on a 16 sensor ULA and the results are tabulated in Table 5.1. The estimation is error-free right down to a half-a-degree separation; however, this good performance deteriorates in the presence of model and estimation errors.

Aliasing: We pointed out earlier (p.211) that the sensor spacing in a ULA must be less than half the wavelength so that there is no aliasing in the frequency-wavenumber spectrum. The same requirement exists in all high resolution methods, namely the Capon spectrum, Maximum entropy spectrum and Music spectrum. The basic reason for aliasing lies in the fact that the direction vector is periodic. Consider anyone column of the matrix $\mathbf{A}$,

$$\mathbf{a}_p(\omega\tau) = col\left\{1, e^{-j\omega_p \frac{d}{c}\sin\theta_p}, e^{-j2\omega_p \frac{d}{c}\sin\theta_p}, \ldots, e^{-j(M-1)\omega_p \frac{d}{c}\sin\theta_p}\right\}$$

Now let $d = \dfrac{\lambda_p}{\sin\theta_p} - \delta_p$ where $0 \le \delta_p \le \dfrac{\lambda_p}{2\sin\theta_p}$, then $\mathbf{a}_p(\omega\tau)$

becomes

$$\mathbf{a}_p(\omega_p \frac{d}{c}\sin\theta_p) = col\left\{1, e^{-j2\pi\frac{d}{\lambda_p}\sin\theta_p}, e^{-j4\pi\frac{d}{\lambda_p}\sin\theta_p}, \ldots, e^{-j(M-1)2\pi\frac{d}{\lambda_p}\sin\theta_p}\right\}$$

$$= col\left\{1, e^{j2\pi\frac{\delta_p}{\lambda_p}\sin\theta_p}, e^{j4\pi\frac{\delta_p}{\lambda_p}\sin\theta_p}, \ldots, e^{j(M-1)2\pi\frac{\delta_p}{\lambda_p}\sin\theta_p}\right\}$$

$$= \mathbf{a}_p(\omega_p \frac{-\delta_p}{c}\sin\theta_p)$$

We can find an angle $\hat{\theta}_p$ such that $\frac{d}{\lambda_p}\sin\hat{\theta}_p = -\frac{\delta_p}{\lambda_p}\sin\theta_p$ and hence

$$\mathbf{a}_p(\omega_p \frac{d}{c}\sin\theta_p) = \mathbf{a}_p(\omega_p \frac{d}{c}\sin\hat{\theta}_p)$$

An aliased spectral peak would appear at $\hat{\theta}_p$ which is related to θ_p,

$$\hat{\theta}_p = \sin^{-1}\left(\frac{\delta_p}{d}\sin\theta_p\right) \tag{5.10}$$

As an example, consider an array with sensor spacing, $\frac{d}{\lambda_p} = 1$ and a wavefront incident at an angle θ_p=60°. For this choice of array and wave parameters $\delta_p = 0.1547$ and from (5.10) we get the angle where the aliased peak will be located, $\hat{\theta}_p = -7.6993°$. The wave number spectrum computed by all four methods is shown in fig. 5.1.

Aliasing is on account of periodicity of a direction vector which in turn is caused by periodicity present in a ULA. Thus, to avoid aliasing, it would be necessary to break this periodicity; for example, we may space the sensors nonuniformly. In a circular array, though sensors are uniformly spaced (e.g. UCA), the time delays are nonuniform; therefore a UCA will yield an alias-free spectrum [4]. This is demonstrated in fig. 5.2 where we consider a wavefront which is incident at 60^{o} (with respect to x-axis) on a circular array consisting of 16 sensors uniformly spread over a circle of radius 8λ. The Capon spectrum is shown for this case. The aliasing phenomenon is not encountered in random arrays where the sensors are spaced at random intervals. But as shown in chapter 2 the random array possesses a highly nonlinear phase response.

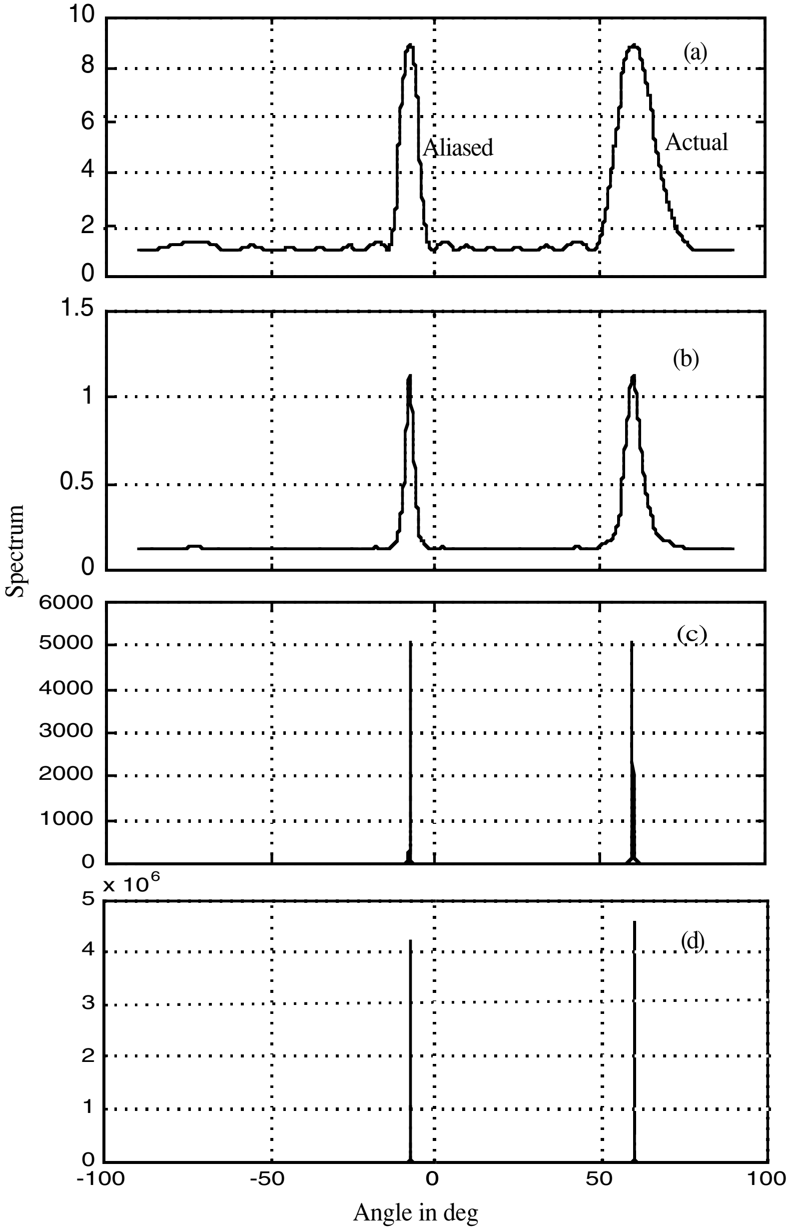

Figure 5.1 The aliasing effect due to undersampling of the wavefield (d=λ). All four methods of spectrum estimation have been used. (a) Bartlett spectrum, (b) Capon spectrum, (c) Maximum entropy spectrum and (d) Music spectrum. While the actual peak is at 60^o the aliased peak appears at -7.69^o.

5.1.2 Correlated Sources: We have so far assumed that the source matrix $\mathbf{S}_0$ is a full rank matrix. When sources are fully uncorrelated $\mathbf{S}_0$ is a diagonal matrix with the nonzero elements representing the power of the sources. The source matrix is naturally full rank. Let us now consider a situation where the sources are partially or fully correlated. We model the source matrix as

$$\mathbf{S}_0 = \mathbf{s}\, \rho\, \mathbf{s}^H \tag{5.11}$$

where

$$\mathbf{s} = diag\left\{\sqrt{s_0}, \sqrt{s_1}, \ldots, \sqrt{s_{P-1}}\right\}$$

$s_0, s_1, \ldots, s_{P-1}$ represent the power of P sources and ρ is the coherence matrix whose (m,n)th element represents the normalized coherence between the mth and nth sources. The signal eigenvalues of the spectral matrix for P=2 are given by [5]

$$\begin{aligned}
\lambda_0 = {} & \frac{M}{2}(s_0 + s_1) + M\sqrt{s_0 s_1}\,\mathrm{Re}\{\rho_{12}\}\psi + \\
& \frac{M}{2}\left\{\left[(s_0 + s_1) + 2\sqrt{s_0 s_1}\,\mathrm{Re}\{\rho_{12}\}\psi\right]^2 - 4 s_0 s_1 (1 - |\psi|^2)(1 - |\rho_{12}|^2)\right\}^{\frac{1}{2}} + \sigma_\eta^2 \\
\lambda_1 = {} & \frac{M}{2}(s_0 + s_1) + M\sqrt{s_0 s_1}\,\mathrm{Re}\{\rho_{12}\}\psi - \\
& \frac{M}{2}\left\{\left[(s_0 + s_1) + 2\sqrt{s_0 s_1}\,\mathrm{Re}\{\rho_{12}\}\psi\right]^2 - 4 s_0 s_1 (1 - |\psi|^2)(1 - |\rho_{12}|^2)\right\}^{\frac{1}{2}} + \sigma_\eta^2
\end{aligned} \tag{5.12a}$$

where

$$\psi(M) = \frac{\sin(\pi \frac{d}{\lambda} M(\sin\theta_0 - \sin\theta_1))}{M \sin(\pi \frac{d}{\lambda}(\sin\theta_0 - \sin\theta_1))}$$

The sum of the signal eigenvalues, that is,

$$\begin{aligned}
&(\lambda_0 - \sigma_\eta^2) + (\lambda_1 - \sigma_\eta^2) = \\
&M(s_0 + s_1) + 2M\sqrt{s_0 s_1}\,\mathrm{Re}\{\rho_{12}\}\psi(M)
\end{aligned} \tag{5.12b}$$

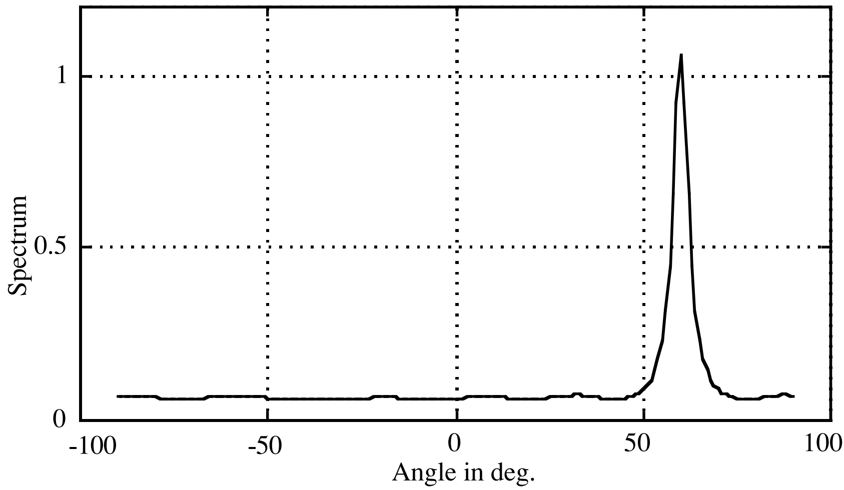

Figure 5.2: No aliasing effect is seen with a circular array. Sixteen sensor UCA with radius= 8λ (sensor spacing=3.12l) is used. A plane wavefront is incident on the array at 60^{o}.

represents coherent addition of power. For uncorrelated sources $\rho_{12} = 0$ (5.12a) reduces to

$$
\begin{aligned}
\lambda_0 &= \frac{M}{2}(s_0 + s_1) + \frac{M}{2}\left\{(s_0 + s_1)^2 - 4s_0 s_1(1 - \left|\psi(M)\right|^2)\right\}^{\frac{1}{2}} + \sigma_\eta^2 \\
\lambda_1 &= \frac{M}{2}(s_0 + s_1) - \frac{M}{2}\left\{(s_0 + s_1)^2 - 4s_0 s_1(1 - \left|\psi(M)\right|^2)\right\}^{\frac{1}{2}} + \sigma_\eta^2
\end{aligned}
\tag{5.13}
$$

Also, note that when the sources are in the same direction $\lambda_0 = M(s_0 + s_1)$ and $\lambda_1 = 0$.

The source spectral matrix may be modified by spatial smoothing of the array outputs. This is achieved by averaging the spectral matrices of subarray outputs over all possible subarrays (see fig. 5.3). The i^{th} subarray (size μ) signal vector at a fixed temporal frequency is given by

$$
\begin{aligned}
\mathbf{F}_i &= col\left\{F_i(\omega), F_{i+1}(\omega), \ldots, F_{i+\mu-1}(\omega)\right\} \qquad 0 \le i \le M - \mu + 1 \\
&= \mathbf{I}_{i,\mu}\mathbf{F}
\end{aligned}
$$

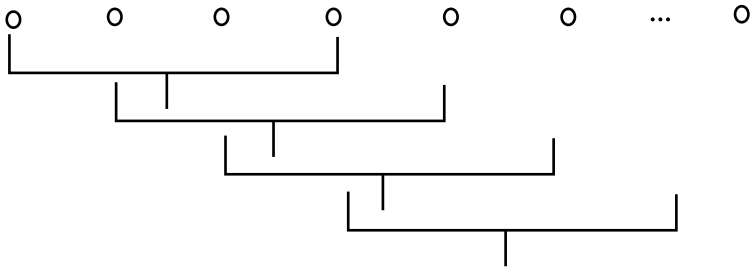

Figure 5.3: Overlapping subarrays are formed as shown above. Each subarray has four sensors. It shares three sensors with its immediate neighbours.

where $\mathbf{I}_{i,\mu}$ is a diagonal matrix,

$$\mathbf{I}_{i,\mu} = diag\left\{\begin{matrix} 0,\ldots 0, & 1,\ldots,1, & 0,\ldots,0 \\ {\scriptstyle 0\ to\ i-1,} & {\scriptstyle i\ to\ i+\mu-1,} & {\scriptstyle i+\mu\ to\ M} \end{matrix}\right\}$$

$$\mathbf{F} = col\{F_0(\omega),\ldots,F_{M-1}(\omega)\}$$

The spectral matrix of the i^{th} subarray is now given by $\mathbf{S}_{i,\mu} = E\{\mathbf{F}_i\mathbf{F}_i^H\} = \mathbf{I}_{i,\mu}\mathbf{S}\ \mathbf{I}_{i,\mu}^H$. We shall now average all subarray spectral matrices

$$\begin{aligned}\overline{\mathbf{S}} &= \frac{1}{M-\mu+1}\sum_{i=0}^{M-\mu+1}\mathbf{S}_{i,\mu} = \frac{1}{M-\mu+1}\sum_{i=0}^{M-\mu+1}\mathbf{I}_{i,\mu}\mathbf{S}\ \mathbf{I}_{i,\mu}^H \\ &= \frac{1}{M-\mu+1}\sum_{i=0}^{M-\mu+1}\mathbf{I}_{i,\mu}\mathbf{A}(\omega)\mathbf{S}_0(\omega)\mathbf{A}^H\ \ \mathbf{I}_{i,\mu}^H + \sigma_\eta^2\mathbf{I}\end{aligned} \tag{5.14a}$$

where we have used the spectral matrix of the signal model plane waves in the presence of white noise (4.12b). We can show that

$$\begin{aligned}&\mathbf{I}_{i,\mu}\mathbf{A}(\omega) = \mathbf{I}_{i,\mu}\left[\mathbf{a}_0,\mathbf{a}_1,\ldots,\mathbf{a}_{P-1}\right] \\ &= \left[\hat{\mathbf{a}}_0,\hat{\mathbf{a}}_1,\ldots,\hat{\mathbf{a}}_{P-1}\right]diag\left\{e^{-j2\pi i\frac{d}{c}\sin\theta_0},\ldots,e^{-j2\pi i\frac{d}{c}\sin\theta_{P-1}}\right\}\end{aligned} \tag{5.14b}$$

where

$$\hat{\mathbf{a}}_i(\omega\tau) = col\left\{1, e^{-j\omega\frac{d}{c}\sin\theta_i}, e^{-j2\omega\frac{d}{c}\sin\theta_i}, \ldots, e^{-j(\mu-1)\omega\frac{d}{c}\sin\theta_i}\right\}$$

We shall use (5.14b) in (5.14a) and obtain

$$\overline{\mathbf{S}} = \hat{\mathbf{A}}\left[\frac{1}{M-\mu+1}\sum_{i=0}^{M-\mu+1}\phi_{\mathrm{i}}\mathbf{S}_0(\omega)\ \phi_{\mathrm{i}}^{\mathrm{H}}\right]\hat{\mathbf{A}}^H + \sigma_\eta^2\mathbf{I} \tag{5.15a}$$

where

$$\hat{\mathbf{A}} = \left[\hat{\mathbf{a}}_0, \hat{\mathbf{a}}_1, \ldots, \hat{\mathbf{a}}_{P-1}\right]$$

$$\phi_{\mathrm{i}} = diag\left\{e^{-j2\pi i\frac{d}{c}\sin\theta_0}, e^{-j2\pi i\frac{d}{c}\sin\theta_1}, \ldots, e^{-j2\pi i\frac{d}{c}\sin\theta_{P-1}}\right\}$$

The quantity inside the square brackets in (5.15a) may be computed by actual multiplication followed by summation,

$$\begin{aligned}[\ ]_{mn} &= \sqrt{s_m s_n}\rho_{mn}\frac{1}{M-\mu+1}\sum_{i=0}^{M-\mu+1} e^{-j2\pi\frac{d}{c}i(\sin\theta_m - \sin\theta_n)} \\ &= \sqrt{s_m s_n}\rho_{mn}\psi(M-\mu+1)e^{-j\pi\frac{d}{c}(M-\mu)(\sin\theta_m-\sin\theta_n)}\end{aligned} \tag{5.15b}$$

From (5.15b) it follows that the coherence after spatial smoothing may be written as

$$\overline{\rho}_{mn} = \rho_{mn}\psi(M-\mu+1)e^{-j\pi\frac{d}{c}(M-\mu)(\sin\theta_m-\sin\theta_n)} \tag{5.16}$$

The magnitude of the off-diagonal terms in the coherence matrix, ρ (see (5.11)), is reduced by a factor, $\psi(M-\mu+1)$, which is indeed small (<<1) for large $(M-\mu+1)$. This contributes to the increase of the rank of the smoothed coherence matrix. It is shown in [6] that ρ becomes full rank when $M-\mu+1 \geq P$.

Let us now examine the effect of the spatial smoothing on the eigenvalues for the two source case. From

$$\bar{\lambda}_0 = \frac{\mu}{2}(s_0 + s_1) + \mu\sqrt{s_0 s_1}\,\mathrm{Re}\{\tilde{\rho}_{01}\}\psi(\mu)\psi(M-\mu+1) +$$

$$\frac{\mu}{2}\left\{\begin{matrix}\left[(s_0 + s_1) + 2\sqrt{s_0 s_1}\,\mathrm{Re}\{\tilde{\rho}_{01}\}\psi(\mu)\psi(M-\mu+1)\right]^2 \\ -4 s_0 s_1 (1 - |\psi(\mu)|^2)(1 - |\rho_{01}\psi(M-\mu+1)|^2)\end{matrix}\right\}^{\frac{1}{2}} + \sigma_\eta^2$$

$$\bar{\lambda}_1 = \frac{\mu}{2}(s_0 + s_1) + \mu\sqrt{s_0 s_1}\,\mathrm{Re}\{\tilde{\rho}_{01}\}\psi(\mu)\psi(M-\mu+1) -$$

$$\frac{\mu}{2}\left\{\begin{matrix}\left[(s_0 + s_1) + 2\sqrt{s_0 s_1}\,\mathrm{Re}\{\tilde{\rho}_{01}\}\psi(\mu)\psi(M-\mu+1)\right]^2 \\ -4 s_0 s_1 (1 - |\psi(\mu)|^2)(1 - |\rho_{01}\psi(M-\mu+1)|^2)\end{matrix}\right\}^{\frac{1}{2}} + \sigma_\eta^2 \tag{5.17}$$

where $\tilde{\rho}_{01} = \rho_{01} e^{j\pi \frac{d}{\lambda}(M-\mu)(\sin\theta_0 - \sin\theta_1)}$. The sum of the signal eigenvalues is given by

$$(\bar{\lambda}_0 - \sigma_\eta^2) + (\bar{\lambda}_1 - \sigma_\eta^2) =$$
$$M(s_0 + s_1) + 2M\sqrt{s_0 s_1}\,\mathrm{Re}\{\tilde{\rho}_{01}\}\psi(\mu)\psi(M-\mu+1)$$

If we select μ such that

$$\pi\frac{d}{\lambda}(M-\mu+1)|(\sin\theta_0 - \sin\theta_1)| \approx \pi$$

then $\psi(M-\mu+1) \approx 0$, $\bar{\lambda}_0 = M s_0$ and $\bar{\lambda}_1 = M s_1$ and the desired subarray size would be

$$\mu \approx (M+1) - \frac{2}{|(\sin\theta_0 - \sin\theta_1)|}$$

Let $|(\sin\theta_0 - \sin\theta_1)| \approx \frac{1}{\mu}$. Then the desired subarray size is

$$\mu \approx \frac{1}{3}(M+1) \tag{5.18}$$

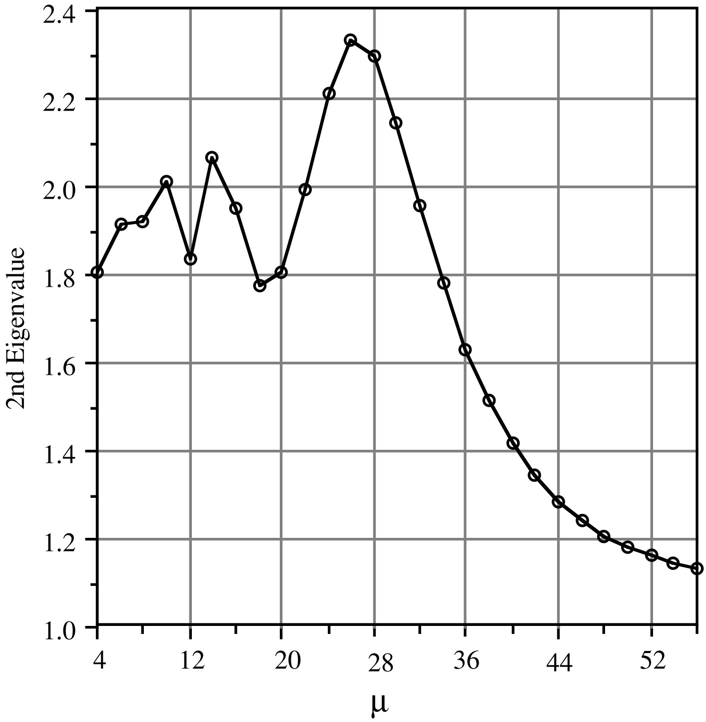

Figure 5.4: The 2nd eigenvalue relative to noise variance is shown as a function of the subarray size (μ).

This result is very close to that given in [7]. We have evaluated $\frac{\bar{\lambda}_1}{\sigma_\eta^2}$ as a function of the subarray size for two perfectly correlated equal power waves incident at angles θ_0 and θ_1 such that $\sin\theta_0 - \sin\theta_1 = \frac{1}{\mu}$ on a ULA with 64 sensors and array snr =10. The results are shown in fig. 5.4.

5.1.3 Direct Estimation: In MUSIC it is required to scan the entire angular range of $\pm\frac{\pi}{2}$. Since the spectral peaks are extremely fine the scanning must be done at a very fine interval; otherwise there is a high risk of missing the peak altogether. This is a serious drawback of the subspace methods based on scanning. Alternatively, there are direct methods which enable us to estimate the DOA directly. We shall describe three such methods, namely, Pisarenko's method, minimum norm, and root Music and show how they are interrelated.

Pisarenko's Method: Let the array size be $M = P + 1$ where P stands for the number of uncorrelated sources. The noise subspace is now spanned by a single eigenvector, $\mathbf{v}_{M-1}$. Hence, the direction vector, $\mathbf{a}$, will be orthogonal to $\mathbf{v}_{M-1}$,

$$\mathbf{v}_{M-1}^H \mathbf{a} = 0 \tag{5.19}$$

The direction vector of the pth source may be expressed as

$$\begin{aligned}\mathbf{a}_p &= col\left\{1, e^{-j2\pi\frac{d}{\lambda}\sin\theta_p}, \ldots, e^{-j2\pi(M-1)\frac{d}{\lambda}\sin\theta_p}\right\} \\ &= col\left\{1, z_p, z_p^2, \ldots, z_p^{M-1}\right\}, \quad p = 0,1,\ldots,P-1\end{aligned}$$

where $z_p = e^{-j2\pi\frac{d}{\lambda}\sin\theta_p}$. Consider a polynomial

$$\mathbf{v}_{M-1}^H \left[1, z, z^2, \ldots, z^{M-1}\right]^T = 0 \tag{5.20}$$

whose roots are indeed $z_0, z_1, \ldots, z_{P-1}$. In the complex plane all roots lie on a unit circle. The angular coordinate of a root is related to the DOA. For example, let the pth root be located at φ_p. Then $\varphi_p = \pi \sin\theta_p$. This method was first suggested by Pisarenko [3], many years before MUSIC was invented !

Root Music: The Pisarenko's method has been extended taking into account the noise space spanned by two or more eigenvectors [8]. The extended version is often known as root Music. Define a polynomial,

$$S(z) = \sum_{m=P}^{M-1} \mathbf{v}_m^H \left[1, z, z^2, \ldots, z^{M-1}\right]^T \tag{5.21}$$

The roots of $S(z)$ or $D(z) = S(z)S(\frac{1}{z})$ lying on the unit circle will correspond to the DOAs of the sources and the remaining M-P roots will fall inside the unit circle (and also at inverse complex conjugate positions outside the circle).

In the minimum norm method a vector $\mathbf{a}$ is found which is a solution of $\mathbf{a}^H \mathbf{S}_f \mathbf{a} = \min$ under the constraint that $\mathbf{a}^H \mathbf{a} = 1$. It turns out that the solution is an eigenvector of $\mathbf{S}_f$ corresponding to the smallest eigenvalue.

Radial coordinate	Angular coordinate (in radians)	Estimation error variance=.01	
		Radial	Angular
33.3162	0.9139	2.4854	-1.8515
2.2755	2.5400	1.5593	-0.7223
1.5793	2.9561	1.3047	-3.0944
0.8500	-1.7578	0.7244	-2.2490
0.8809	-0.9386	0.9336	1.6835
1.0000	0.5455	1.0050	0.5647
1.0000	0.7600	1.0057	0.7864

Table 5.2: Direct estimation of DOA by computing signal zeros of a polynomial given by (5.20) or (5.21). The results shown in columns one and two are for error free spectral matrix and those in columns three and four are for a spectral matrix with random errors (zero mean and 0.01 variance).

Thus, the minimum norm method belongs to the same class of direct methods of DOA estimation initiated by Pisarenko [3]. An example of DOA obtained by computing zeros on the unit circle under the ideal condition of no errors in the spectral matrix is shown in table 5.2. Two equal power signal wavefronts are assumed to be incident on eight sensor ULA at angles 10^o and 14^o. The DOA estimates from the error-free spectral matrix are exact (columns one and two in table 5.2), but in the presence of even a small error in the estimate of the spectral matrix, a significant error in DOA estimation may be encountered (see columns three and four in the table).

The zeros of the polynomial defined in any one of the above methods are important from the point of DOA estimation. In particular, the zeros which fall on the unit circle or close to it represent the DOAs of the incident wavefronts. These zeros are often called signal zeros and the remaining zeros, located deep inside the unit circle, are called the noise zeros. In MUSIC, a peak in the spectrum represents the DOA of the wavefront. But the height of the peak is greatly influenced by the position of the signal zero. The peak is infinite when the zero is right on the unit circle but it rapidly diminishes when the zero moves away from the unit circle. The peak may be completely lost, particularly in the presence of another signal zero in the neighborhood but closer to the unit circle. Hence, it is possible that, while the spectral peaks remain unresolved, the signal zeros are well separated. The shift of the signal zero may be caused by errors in the estimation of the spectral matrix from finite data. Let a signal zero at z_i be displaced to $\hat{z}_i$. The displacement, both radial and angular, is given by

$$\Delta z_i \approx (z_i - \hat{z}_i) \approx \delta r \, e^{j(u+\delta u)}$$

where we have assumed that $\delta u << 1$. Perturbation analysis reported in [9] for time series shows that the mean square error in δr and δu are related

$$\frac{E\left\{\left|\delta r_i\right|^2\right\}}{E\left\{\left|\delta \theta_i\right|^2\right\}} = 2N\left(\frac{\cos(\theta_i)}{\frac{\omega d}{c}}\right)^2 \leq \frac{2N}{\pi^2} \tag{5.22}$$

where N stand for the number of time samples (or snapshots). From (5.22) it follows that $E\left\{\left|\delta r_i\right|^2\right\} >> E\left\{\left|\delta \theta_i\right|^2\right\}$, particularly when the wavefronts are incident close to broadside. On account of the above finding the magnitude of a spectral peak in MUSIC is likely to be more adversely affected by the errors due to finite data.

Subspace Rotation: The direct estimation of DOA discussed in the previous section requires a ULA. This itself is a restriction in many practical situations. A new principle of DOA estimation, known as subspace rotation, exploits a property of a dipole sensor array, where all dipoles are held in the same direction, which is the subspace spanned by the direction vectors pertaining to the upper sensors in the dipole array and those pertaining to lower sensors are related through a rotation. The principle is explained in chapter 2 (see page 120). The basic starting equation is (2.57), which we reproduce here for convenience,

$$\mathbf{S}_{\tilde{f}} = \begin{bmatrix} \mathbf{A} \\ \mathbf{A\Gamma} \end{bmatrix} \mathbf{S}_f \begin{bmatrix} \mathbf{A} \\ \mathbf{A\Gamma} \end{bmatrix}^H + \begin{bmatrix} \mathbf{I} & \mathbf{0} \\ \mathbf{0} & \mathbf{I} \end{bmatrix} \begin{bmatrix} \sigma^2_{\eta_1} & \\ & \sigma^2_{\eta_2} \end{bmatrix} \tag{2.57}$$

where $\mathbf{S}_{\tilde{f}}$ is the spectral matrix of the dipole array sensors,

$$\mathbf{S}_{\tilde{f}} = \begin{bmatrix} \mathbf{S}_{f_1 f_1} & \mathbf{S}_{f_1 f_2} \\ \mathbf{S}_{f_2 f_1} & \mathbf{S}_{f_2 f_2} \end{bmatrix} = \begin{bmatrix} \mathbf{A}\mathbf{S}_f\mathbf{A}^{\mathrm{H}} & \mathbf{A}\mathbf{S}_f\mathbf{\Gamma}^{\mathrm{H}}\mathbf{A}^{\mathrm{H}} \\ \mathbf{A\Gamma}\mathbf{S}_f\mathbf{A}^{\mathrm{H}} & \mathbf{A}\mathbf{S}_f\mathbf{A}^{\mathrm{H}} \end{bmatrix}$$

Note that $\mathbf{S}_{f_1 f_1}$ is the spectral matrix of the upper sensor outputs and $\mathbf{S}_{f_2 f_2}$ is the spectral matrix of the lower sensor outputs. $\mathbf{S}_{f_1 f_2}$ is the cross-spectral matrix between the upper sensor and lower sensor outputs. From the eigenvalues of $\mathbf{S}_{f_1 f_1}$ we can estimate the noise variance $\sigma^2_{\eta_1}$ (and $\sigma^2_{\eta_2}$ from $\mathbf{S}_{f_2 f_2}$) and subtract it from the spectral matrix. Define $\mathbf{S}^0_{f_1 f_1} = \mathbf{S}_{f_1 f_1} - \sigma^2_{\eta_1}$. Consider the generalized eigenvector (GEV) problem of the matrix pencil $\left\{\mathbf{S}^0_{f_1 f_1}, \mathbf{S}_{f_1 f_2}\right\}$,

$$\mathbf{S}^0_{f_1 f_1}\mathbf{v} = \gamma \mathbf{S}_{f_1 f_2}\mathbf{v} \tag{5.23}$$

where γ is a generalized eigenvalue and $\mathbf{v}$ is a corresponding eigenvector. Consider the following:

$$\begin{aligned}
\mathbf{v}^H\left[\mathbf{S}^0_{f_1 f_1} - \gamma \mathbf{S}_{f_1 f_2}\right]\mathbf{v} &= \mathbf{v}^H\left[\mathbf{A}\mathbf{S}_f\mathbf{A}^H - \gamma \mathbf{A}\mathbf{S}_f\boldsymbol{\Gamma}^H\mathbf{A}^H\right]\mathbf{v} \\
&= \mathbf{v}^H\mathbf{A}\mathbf{S}_f\left[\mathbf{I} - \gamma\boldsymbol{\Gamma}^H\right]\mathbf{A}^H\mathbf{v} \\
&= \mathbf{v}^H\mathbf{A}\mathbf{S}_f\left[\mathbf{I} - \gamma\boldsymbol{\Gamma}^H\right]\mathbf{A}^H\mathbf{v} \\
&= \mathbf{v}^H\mathbf{Q}\mathbf{v} = 0
\end{aligned} \tag{5.24}$$

Since $\mathbf{S}_f$ is full rank as the sources are assumed to be uncorrelated and $\mathbf{A}$ is assumed to be full rank, then, for the right hand side of (5.24) to be true, we must have $\gamma = e^{-j\frac{\omega}{c}\Delta.\delta_i}$. The rank of $\mathbf{Q}$ will be reduced by one and a vector $\mathbf{v}$ can be found to satisfy (5.24). Thus the generalized eigenvalues of the matrix pencil $\left\{\mathbf{S}^0_{f_1 f_1}, \mathbf{S}_{f_1 f_2}\right\}$ are $\gamma_i = e^{-j\frac{\omega}{c}\Delta.\delta_i}, i = 0,1,\ldots,P-1$ from which we can estimate $\theta_i, i = 0,1,\ldots,P-1$. This method of DOA estimation is known as ESPRIT (Estimation of signal parameters via rotation invariance technique) [10]. An example of DOA obtained via ESPRIT is in table 5.3. The eigenvalues of the pencil matrix (5.23) under the ideal condition of no errors in the spectral matrix as well as with errors in the spectral matrix are shown in table 5.3. Two equal power signal wavefronts are assumed to be incident on eight sensor ULA at angles 10° and 14°. The eigenvalues estimated from error free spectral matrix are exact (columns one and two in table 5.3), but in the presence of a small error in the estimation of the spectral matrix, a significant error in DOA estimation may be encountered (see columns three and four in the table).

The generalized eigenvector $\mathbf{v}_i$, corresponding to eigenvalue γ_i, possesses an interesting property. Let us write (5.24) in expanded form

Radial coordinate	Angular coordinate (in radians)	Estimation error variance=.01	
		Radial	Angular
4.6642	1.8540	3.4640	-2.1554
2.0198	0.7276	2.5202	0.4402
0.8182	-2.3272	1.7050	-0.4834
0.2108	-2.6779	0.5738	-1.6783
0.5224	-0.3753	0.4586	1.6290
0.5193	1.1199	0.6753	0.9060
1.0000	0.5455	0.9969	0.5533
1.0000	0.7600	1.0087	0.7720

Table 5.3: Generalized eigenvalues of pencil matrix (5.23).

$$\left[\mathbf{v}_i^H\mathbf{a}_0,\ldots,\mathbf{v}_i^H\mathbf{a}_{i-1},\mathbf{v}_i^H\mathbf{a}_{i+1},\ldots,\mathbf{v}_i^H\mathbf{a}_{P-1}\right]\hat{\mathbf{S}}_f \begin{bmatrix} 1-\gamma_i e^{j\frac{\omega d}{c}\sin\theta_0} & \cdots & 0 \\ & & \\ 0 & \cdots & 1-\gamma_i e^{j\frac{\omega d}{c}\sin\theta_{P-1}} \end{bmatrix} \begin{bmatrix} \mathbf{v}_i^H\mathbf{a}_0 \\ \cdot \\ \cdot \\ \cdot \\ \mathbf{v}_i^H\mathbf{a}_{i-1,} \\ \mathbf{v}_i^H\mathbf{a}_{i+1} \\ \cdot \\ \cdot \\ \cdot \\ \mathbf{v}_i^H\mathbf{a}_{P-1} \end{bmatrix} = 0$$

where $\hat{\mathbf{S}}_f$ represents the source matrix where the i$^{\text{th}}$ column and the i$^{\text{th}}$ row are deleted. Since $\gamma_i \neq e^{-j\frac{\omega_0}{c}\Delta.\delta_k}, i \neq k$, the diagonal matrix will be full rank and also $\hat{\mathbf{S}}_f$ is full rank by assumption, we must have $\mathbf{v}_i^H\mathbf{a}_{k,} = 0$ for all $k \neq i$. Thus, the generalized signal eigenvector of the pencil matrix $\left\{\mathbf{S}_{f_1 f_1}^0, \mathbf{S}_{f_1 f_2}\right\}$ is orthogonal to all direction vectors except the i$^{\text{th}}$ direction vector. We shall exploit this property for signal separation and estimation later in chapter 6.

5.1.4 Diffused Source: A point source, on account of local scattering or fluctuating medium or reflections from an uneven surface, may appear as a diffused source, that is, the main source surrounded by many secondary sources. A sensor array will receive a large number of rays, all of which would have actually started from the same point (main source) but have traveled different paths due to scattering or refraction or reflection. Such a model was considered in chapter 1 (p. 49). Here we shall explore the possibilities of localizing such a diffused source, in particular, a diffused source due to local scattering (see fig. 1.29). The model of the diffused source signal is given by (1.65)

$$\mathbf{f}(t) = \tilde{\mathbf{a}} s(t) + \eta(t) \tag{5.25}$$

where $\tilde{\mathbf{a}} = \sum_{l=0}^{L-1} \alpha_l e^{-j\omega_c \delta t_l} \mathbf{a}(\theta + \delta\theta_l)$ where α_l, δt_l and $\delta\theta_l$ are for the lth ray, complex amplitude, time delay and direction of arrival with respect to a direct ray from the main source, respectively. Assume that there are L rays reaching the sensor array. For the direct ray we shall assume that $\alpha_0 = 1$, $\delta t_0 = 0$ and $\delta\theta_0 = 0$. The covariance matrix of the array (ULA) output is given by (see eq. 1.70)

$$\mathbf{c}_f \approx \sigma_s^2 L \sigma_\alpha^2 \mathbf{D}(\theta) \mathbf{Q} \mathbf{D}^H(\theta) + \sigma_\eta^2 \mathbf{I} \tag{5.26}$$

where we have assumed that the scatterers are uniformly distributed in the angular range $\pm\Delta$. The $\mathbf{Q}$ matrix for the assumed uniform distribution is given by

$$\{\mathbf{Q}\}_{mn} = \frac{\sin 2\pi \frac{d}{\lambda}(m-n)\Delta\cos\theta}{2\pi\frac{d}{\lambda}(m-n)\Delta\cos\theta}$$

and

$$\mathbf{D} = diag\left[1, e^{j\frac{2\pi d}{\lambda}\sin\theta}, \ldots, e^{j\frac{2\pi(M-1)d}{\lambda}\sin\theta}\right]$$

The eigendecomposition of $\mathbf{Q}$ shows some interesting properties [11]. There are r, where $r = \left[2\frac{d}{\lambda} M\Delta\cos\theta\right]$, significant eigenvalues close to unity ([x] stands for the largest integer greater than x). The remaining (M-r) eigenvalues are insignificant. Let $\mathbf{v}_\eta$ be a matrix whose columns are M-r eigenvectors corresponding to M-r insignificant eigenvalues (cf. the noise subspace in the Music algorithm). Now it follows that

$$\mathbf{v}_\eta^H \left[\mathbf{c}_f - \sigma_\eta^2 \mathbf{I}\right] \mathbf{v}_\eta = \mathbf{0} \quad \text{(a matrix M-r x M-r zeros)} \tag{5.27}$$

Using (5.26) in (5.27) we obtain

$$\sigma_s^2 L \sigma_\alpha^2 \sum_{m=0}^{r-1} \lambda_m \mathbf{v}_\eta^H \mathbf{D}(\theta) \mathbf{e}_m \mathbf{e}_m^H \mathbf{D}^H(\theta) \mathbf{v}_\eta = \mathbf{0} \tag{5.28}$$

where we have used eigendecomposition of $\mathbf{Q} \approx \sum_{m=0}^{r-1} \lambda_m \mathbf{e}_m \mathbf{e}_m^H$. Here λ_m (≈ 1) are significant eigenvalues of $\mathbf{Q}$. Since $\sigma_{f_0}^2$, and λ_m >0 for all m<r, the following must hold good for all m<r:

$$\left|\mathbf{v}_\eta^H \mathbf{D}(\theta) \mathbf{e}_m\right|^2 = 0 \tag{5.29}$$

for all m<r. The azimuth of the center of the cluster can be estimated using the orthogonality property demonstrated in (5.29). The eigenvectors $\mathbf{e}_m$, discrete prolate spheroidal sequence (DPSS), are obtained by eigendecomposition of the $\mathbf{Q}$ matrix. But in $\mathbf{Q}$ there is an unknown parameter pertaining to the width of the cluster, namely, $\Delta \cos\theta$ which has to be estimated. We have in chapter 1 (page 59) indicated that the rank of the covariance matrix (noise free) is closely related to this unknown parameter.

5.1.5 Adaptive Subspace: Adaptive methods for the estimation of the eigenvector corresponding to the minimum (or maximum) eigenvalue have been described by many researchers[12-14]. The method is based on inverse power iteration [15]

$$\begin{aligned} \hat{\mathbf{v}}^0 &= [1,0,\ldots,0]^T \\ \tilde{\mathbf{v}}^{k+1} &= \mathbf{S}_f^{-1}(\omega) \hat{\mathbf{v}}^k \\ \hat{\mathbf{v}}^{k+1} &= \frac{\tilde{\mathbf{v}}^{k+1}}{\sqrt{\tilde{\mathbf{v}}^{k+1^T} \tilde{\mathbf{v}}^{k+1}}} \end{aligned} \tag{5.30}$$

where $\hat{\mathbf{v}}^k$ is an eigenvector at k$^{\text{th}}$ iteration and the last equation is meant for normalization. To estimate the eigenvector corresponding to the largest eigenvalue the algorithm shown in (5.30) may be used with the difference that the spectral matrix, instead of its inverse, is used.

An attempt to extend the inverse power iteration method to the estimation of the entire subspace (signal or noise subspace) has also been reported [13]. All the above methods require computation of the gradient of a cost function which is minimized. The gradient computation is slow; furthermore, in the presence of noise, it is unstable. Additionally, the rate of convergence of a gradient method is known to be very slow [14]. The alternate approach is to use the well-known power method for estimation of an eigenvector corresponding to the minimum (or maximum) eigenvalue [15]. The power method is easy to understand and easy to implement on a computer. We shall briefly describe the power method for estimation of the entire signal or noise subspace. Let $\hat{\mathbf{v}}_m^N, m = 1,2,\ldots P$ be the eigenvectors based on the data till time N, that is, the eigenvectors of the spectral matrix, $\hat{\mathbf{S}}_f^N(\omega)$. When a new sample arrives the eigenvectors are updated using the following recursive equation followed by Gram-Schmidt orthonormalization (GSO),

$$\begin{aligned} &\hat{\mathbf{S}}_f^{N+1}\hat{\mathbf{v}}_m^N = \mathbf{g}_m^{N+1} \\ &\hat{\mathbf{v}}_m^{N+1} = GSO\left\{\mathbf{g}_m^{N+1}\right\}, \quad m = 1,2,\ldots P \end{aligned} \tag{5.31}$$

The choice of initial eigenvectors to start the recursion is important for rapid convergence. A suggested choice in [14] is to orthonormalize P initial frequency snapshots and use them as the initial eigenvectors. The starting value of the spectral matrix is chosen as

$$\hat{\mathbf{S}}_f^P = (\mathbf{I} + \mathbf{F}_0\mathbf{F}_0^H)$$

The Gram-Schmidt orthonormalization process involves finding p orthonormal vectors which are linearly equivalent to data vectors [50]. Let $\mathbf{F}_1, \mathbf{F}_2, \ldots, \mathbf{F}_P$ be a set of frequency snapshots and $\mathbf{I}_1, \mathbf{I}_2, \ldots, \mathbf{I}_P$ be the set of linearly equivalent orthonormal vectors which satisfy the following conditions

$$\mathbf{I}_k \perp \mathbf{F}_r \;\; for\ r < k$$

$$\left|\mathbf{I}_k\right|^2 = 1 \;for\ all\ k \tag{5.32}$$

The Gram-Schmidt method determines the orthonormal vectors by solving a system of linear equations

$$
\begin{aligned}
&\mathbf{I}_1 = \gamma_1^1\mathbf{F}_1 \\
&\mathbf{I}_2 = \gamma_1^2\mathbf{F}_1 + \gamma_2^2\mathbf{F}_2 \\
&\mathbf{I}_3 = \gamma_1^2\mathbf{F}_1 + \gamma_2^2\mathbf{F}_2 + \gamma_3^2\mathbf{F}_3 \\
&\ldots \\
&\mathbf{I}_P = \gamma_1^P\mathbf{F}_1 + \gamma_2^P\mathbf{F}_2 + \ldots + \gamma_P^P\mathbf{F}_P
\end{aligned}
\tag{5.33}
$$

§5.2 **Subspace Methods** (Broadband):

Since the location parameters are independent of frequency, we ought to get identical location estimates at different frequencies. But, on account of errors in the estimation of the spectral matrix, the location estimates are likely to be different at different frequencies. The errors in the estimation of a spectral matrix are likely to be uncorrelated random variables. By suitably combining the spectral matrix estimates obtained at different frequencies, it is hoped that the error in the final location estimate can be reduced. This is the motivation for broadband processing. In the process of combining all spectral matrices it is important that the basic structure of the spectral matrices should not be destroyed. For example, a spectral matrix at all signal frequencies is of rank one when there is only one source or rank two when there are two uncorrelated sources, and so on. Consider a ULA and a single source. The spectral matrix at frequency ω is given by $\mathbf{S}(\omega) = \mathbf{a}(\omega,\theta)S_0(\omega)\mathbf{a}^H(\omega,\theta) + \sigma_\eta^2\mathbf{I}$. Notice that the frequency dependence of direction vectors is explicitly shown. Let us consider a generalized linear transformation of the form, $\mathbf{T}(\omega)\mathbf{S}(\omega)\mathbf{T}^H(\omega)$, where $\mathbf{T}(\omega)$ is a transformation matrix, yet to be chosen. The transformation matrix must map the direction vector into another direction vector at a chosen frequency and the background noise continues to remain white. The transformed spectral matrix is given by

$$
\begin{aligned}
&\mathbf{T}(\omega)\mathbf{S}(\omega)\mathbf{T}^H(\omega) = \\
&\mathbf{T}(\omega)\mathbf{a}(\omega,\theta)S_0(\omega)\mathbf{a}^H(\omega,\theta)\mathbf{T}^H(\omega) + \sigma_\eta^2\mathbf{T}(\omega)\mathbf{T}^H(\omega)
\end{aligned}
\tag{5.34}
$$

where the transformation matrix $\mathbf{T}(\omega)$ must possess the following properties:

$$
\begin{aligned}
&\mathbf{T}(\omega)\mathbf{a}(\omega,\theta) = \mathbf{a}(\omega_0,\theta) \\
&\mathbf{T}(\omega)\mathbf{T}^H(\omega) = \mathbf{I}
\end{aligned}
\tag{5.35}
$$

where ω_0 is a selected frequency. Using (5.35) in (5.34) and averaging over a band of frequencies we obtain

$$\begin{aligned}\overline{\mathbf{S}}(\omega_0) &= \sum_{i \in bw} \mathbf{T}(\omega_i)\mathbf{S}(\omega_i)\mathbf{T}^H(\omega_i) \\ &= \mathbf{a}(\omega_0,\theta)\sum_{i \in bw} S_0(\omega_i)\mathbf{a}^H(\omega_0,\theta) + \sigma_\eta^2\mathbf{I} \end{aligned} \tag{5.36}$$

where bw stands for the signal bandwidth. In (5.36) we observe that the signal power spread over a band of frequencies has been focused at one frequency, namely, ω_0. This idea of focusing of energy has been actively pursued in [16, 17] for DOA estimation.

In the direction vector there is a parameter, namely, sensor spacing which may be changed according to the frequency such that $\frac{\omega d}{c}$ remains constant. This will require the sensor spacing at frequency ω_i should be equal to $d_i = \frac{\omega_0 d_0}{\omega_i}, i \in bw$. In practice the required change in the physical separation is difficult to achieve, but resampling of the wavefield through interpolation is possible. This approach to focusing was suggested in [18]. In chapter 2 we introduced the spatio temporal covariance matrix (STCM) which contains all spatio temporal information present in a wavefield. It has been extensively used for source localization [19]. We shall probe into the signal and noise subspace structure of STCM of ULA as well as UCA and show how the structure can be exploited for source localization.

5.2.1 Wideband Focusing: Consider P uncorrelated point sources in a far field and a ULA for DOA estimation. As in (4.12b) the spectral matrix of an array signal may be expressed as $\mathbf{S}_f(\omega) = \mathbf{A}(\omega,\theta)\mathbf{S}_0(\omega)\mathbf{A}^H(\omega,\theta)$ where the columns of $\mathbf{A}(\omega,\theta)$ matrix are the direction vectors. We seek a transformation matrix $\mathbf{T}(\omega)$ which will map the direction vectors at frequency ω into direction vectors at the preselected frequency ω_0 as in (5.35). There is no unique solution but a least squares solution is possible,

$$\mathbf{T}(\omega) \approx \mathbf{A}(\omega_0,\theta)\left[\mathbf{A}^H(\omega,\theta)\mathbf{A}(\omega,\theta)\right]^{-1}\mathbf{A}^H(\omega,\theta) \tag{5.37}$$

The transformation matrix given by (5.37) depends upon the unknown azimuth information. However, it is claimed in [20] that approximate estimates obtained through beamformation or any other simple approach are adequate. As an example, consider a single source case. For this, $\mathbf{A}(\omega,\theta) =$

$col\left\{1, e^{-j\omega\frac{d}{c}\sin\theta}, \ldots, e^{-j\omega(M-1)\frac{d}{c}\sin\theta}\right\}$ and the transformation matrix given by (5.37) is equal to $\mathbf{T}(\omega) \approx \frac{1}{N}\mathbf{A}(\omega_0,\theta)\mathbf{A}^H(\omega,\theta)$. To show that this is not a unique answer, consider the following transformation matrix,

$$\mathbf{T}(\omega) = diag\left\{1, e^{-j(\omega_0-\omega)\frac{d}{c}\sin\theta}, \ldots, e^{-j(\omega_0-\omega)(M-1)\frac{d}{c}\sin\theta}\right\} \quad (5.38a)$$

Clearly, using (5.38a) we can also achieve the desired transformation. In (5.38a) let ω_0=0; the transformation matrix becomes

$$\mathbf{T}(\omega) = diag\left\{1, e^{j\omega\frac{d}{c}\sin\theta}, \ldots, e^{j\omega(M-1)\frac{d}{c}\sin\theta}\right\} \quad (5.38b)$$

which we shall use as a filter on the array output. The filtered output is given by

$$\begin{aligned}\mathbf{f}_1(t) &= \frac{1}{2\pi}\int_{-\infty}^{\infty}\mathbf{T}(\omega)\mathbf{F}(\omega)e^{j\omega t}d\omega \\ &= col\left\{f(t), f(t-\frac{d}{c}\sin\theta), \ldots, f(t-\frac{d}{c}(M-1)\sin\theta)\right\}\end{aligned} \quad (5.39)$$

which indeed is the same as the progressively delayed array output in beamformation processing. Let us next compute the covariance function of the filtered output,

$$\begin{aligned}\mathbf{c}_{f_1} &= E\left\{\mathbf{f}_1(t)\mathbf{f}_1^H(t)\right\} \\ &= E\left\{\begin{matrix}\left[f(t-m\frac{d}{c}\sin\theta), m=0,1,\ldots,M-1\right] \\ \left[f(t-m\frac{d}{c}\sin\theta), m=0,1,\ldots,M-1\right]^H\end{matrix}\right\} \\ &= \mathbf{c}_f((m-n)\frac{d}{c}(\sin\theta_0 - \sin\theta)) = \left[\mathbf{c}_f\right]_{mn}\end{aligned}$$

where $\mathbf{c}_f$ is the covariance matrix of the signal emitted by the source. $\mathbf{c}_{f_1}$ is known as the steered covariance matrix [21]. When $\theta = \theta_0$ all elements of $\mathbf{c}_{f_1}$ are equal to a constant equal to the total signal power, that is, $\frac{1}{2\pi}\int_{-\infty}^{\infty} S_f(\omega)d\omega$. Thus, in beamformation we seem to focus all signal power to zero frequency. When there is more than one source we should compute a series of steered covariance matrices over a range of azimuth angles. Whenever a steering angle matches with one of the directions of arrival the steered covariance matrix will display a strong 'dc' term, equal to the power of the source.

The main drawback of wideband focusing is the requirement that the DOAs of incident wavefronts must be known, at least approximately, but the resulting estimate is likely to have large bias and variance [20]. To overcome this drawback an alternate approach has been suggested in [22]. Let $\mathbf{A}$ and $\mathbf{B}$ be two square matrices and consider a two sided transformation, $\mathbf{TBT}^H$, which is closest to $\mathbf{A}$. It is shown in [22] that this can be achieved if $\mathbf{T} = \mathbf{v}_A \mathbf{v}_B^H$ where $\mathbf{v}_A$ is a matrix whose columns are eigenvectors of $\mathbf{A}$ and $\mathbf{v}_B$ is similarly the eigenvector matrix of $\mathbf{B}$. Now let $\mathbf{A}$ and $\mathbf{B}$ be the spectral matrices at two frequencies, $\mathbf{A} = \mathbf{S}_f(\omega_0)$ and $\mathbf{B} = \mathbf{S}_f(\omega_i)$. To transform $\mathbf{S}_f(\omega_i)$ into $\mathbf{S}_f(\omega_0)$ the desired matrix is

$$\mathbf{T}(\omega_0, \omega_i) = \mathbf{v}_s(\omega_0)\mathbf{v}_s^H(\omega_i) \tag{5.40}$$

where $\mathbf{v}_s$ is a matrix whose columns are signal eigenvectors. It is easy to show that $\mathbf{T}(\omega_0, \omega_i)\mathbf{T}^H(\omega_0, \omega_i) = \mathbf{I}$. Applying the transformation on a spectral matrix at frequency ω_i we get

$$\begin{aligned}
&\mathbf{T}(\omega_0, \omega_i)\mathbf{S}_f(\omega_i)\mathbf{T}^H(\omega_0, \omega_i) \\
&= \mathbf{v}_s(\omega_0)\mathbf{v}_s^H(\omega_i)\mathbf{S}_f(\omega_i)\mathbf{v}_s(\omega_i)\mathbf{v}_s^H(\omega_0) \\
&= \mathbf{v}_s(\omega_0)\lambda(\omega_i)\mathbf{v}_s^H(\omega_0)
\end{aligned}$$

where

$$\lambda(\omega_i) = diag\{\lambda_0(\omega_i), \lambda_1(\omega_i), \ldots, \lambda_{P-1}(\omega_i), 0, \ldots, 0\},$$

are the eigenvalues of the noise free spectral matrix, $\mathbf{S}_f(\omega_i)$. Next, we average all transformed matrices and show that

$$
\begin{aligned}
\overline{\mathbf{S}}_f(\omega_0) &= \frac{1}{N}\sum_{i=1}^{N}\mathbf{T}(\omega_0,\omega_i)\mathbf{S}_f(\omega_i)\mathbf{T}^H(\omega_0,\omega_i) \\
&= \mathbf{v}_s(\omega_0)\frac{1}{N}\sum_{i=1}^{N}\lambda(\omega_i)\mathbf{v}_s^H(\omega_0) \\
&= \mathbf{v}_s(\omega_0)\overline{\lambda}\mathbf{v}_s^H(\omega_0)
\end{aligned}
\tag{5.41}
$$

$\overline{\mathbf{S}}_f(\omega_0)$ is the focused spectral matrix whose eigenvectors are the same as those of $\mathbf{S}_f(\omega_0)$ (before focusing) but its eigenvalues are equal to the averaged eigenvalues of all spectral matrices taken over the frequency band. We may now use the focused spectral matrix for DOA estimation.

5.2.2 Spatial Resampling: The basic idea is to resample the wavefield sensed by a fixed ULA so as to create a virtual ULA with a different sensor spacing depending upon the frequency. The spectral matrices computed at different frequencies are then simply averaged. Let us take a specific case of two wideband uncorrelated sources in the far field. The spectral matrix is given by

$$
\mathbf{S}_f(\omega) = \begin{bmatrix}
\mathbf{a}(\omega\frac{d}{c}\sin\theta_0)S_0(\omega)\mathbf{a}^H(\omega\frac{d}{c}\sin\theta_0) + \\
\mathbf{a}(\omega\frac{d}{c}\sin\theta_1)S_1(\omega)\mathbf{a}^H(\omega\frac{d}{c}\sin\theta_1)
\end{bmatrix} + \sigma_\eta^2\mathbf{I}
$$

where $S_0(\omega)$ and $S_1(\omega)$ are spectra of the first and the second source respectively. We compute the spectral matrix at two different frequencies, ω_0 and ω_1, with different sensor spacings, d_0 and d_1, where

$$
d_1 = d_0\frac{\omega_0}{\omega_1}
$$

and form a sum.

$$
\mathbf{S}_f(\omega_0) + \mathbf{S}_f(\omega_1) =
$$

$$
\left\{\begin{matrix}
\mathbf{a}(\omega_0\frac{d_0}{c}\sin\theta_0)S_0(\omega_0)\mathbf{a}^H(\omega_0\frac{d_0}{c}\sin\theta_0) \\
+\mathbf{a}(\omega_0\frac{d_0}{c_0}\sin\theta_1)S_1(\omega_0)\mathbf{a}^H(\omega_0\frac{d_0}{c}\sin\theta_1)
\end{matrix}\right\} + \sigma_\eta^2\mathbf{I}
$$

$$
+\begin{Bmatrix} \mathbf{a}(\omega_1 \frac{d_1}{c}\sin\theta_0)S_0(\omega_1)\mathbf{a}^H(\omega_1 \frac{d_1}{c}\sin\theta_0) \\ +\mathbf{a}(\omega_1 \frac{d_1}{c}\sin\theta_1)S_1(\omega_1)\mathbf{a}^H(\omega_1 \frac{d_1}{c}\sin\theta_1) \end{Bmatrix} + \sigma_\eta^2\mathbf{I}
$$

$$
= \mathbf{a}(\omega_0 \frac{d_0}{c}\sin\theta_0)\left[S_0(\omega_0)+S_0(\omega_i)\right]\mathbf{a}^H(\omega_0 \frac{d_0}{c}\sin\theta_0)
$$

$$
+\mathbf{a}(\omega_0 \frac{d_0}{c}\sin\theta_1)\left[S_1(\omega_0)+S_1(\omega_i)\right]\mathbf{a}^H(\omega_0 \frac{d_0}{c}\sin\theta_1) + 2\sigma_\eta^2\mathbf{I}
$$

$$
\mathbf{S}_f(\omega_0)+\mathbf{S}_f(\omega_1) =
$$

$$
\begin{Bmatrix} \mathbf{a}(\omega_0 \frac{d_0}{c}\sin\theta_0)S_0(\omega_0)\mathbf{a}^H(\omega_0 \frac{d_0}{c}\sin\theta_0) \\ +\mathbf{a}(\omega_0 \frac{d_0}{c\;0}\sin\theta_1)S_1(\omega_0)\mathbf{a}^H(\omega_0 \frac{d_0}{c}\sin\theta_1) \end{Bmatrix} + \sigma_\eta^2\mathbf{I}
$$

$$
+\begin{Bmatrix} \mathbf{a}(\omega_1 \frac{d_1}{c}\sin\theta_0)S_0(\omega_1)\mathbf{a}^H(\omega_1 \frac{d_1}{c}\sin\theta_0) \\ +\mathbf{a}(\omega_1 \frac{d_1}{c}\sin\theta_1)S_1(\omega_1)\mathbf{a}^H(\omega_1 \frac{d_1}{c}\sin\theta_1) \end{Bmatrix} + \sigma_\eta^2\mathbf{I} \tag{5.42}
$$

$$
= \mathbf{a}(\omega_0 \frac{d_0}{c}\sin\theta_0)\left[S_0(\omega_0)+S_0(\omega_i)\right]\mathbf{a}^H(\omega_0 \frac{d_0}{c}\sin\theta_0)
$$

$$
+\mathbf{a}(\omega_0 \frac{d_0}{c}\sin\theta_1)\left[S_1(\omega_0)+S_1(\omega_i)\right]\mathbf{a}^H(\omega_0 \frac{d_0}{c}\sin\theta_1) + 2\sigma_\eta^2\mathbf{I}
$$

Let us assume that N virtual arrays, each with different sensor spacing, have been created by a resampling process. We can generalize (5.42),

$$
\begin{aligned}
\frac{1}{N}\sum_{i=0}^{N-1}\mathbf{S}_f(\omega_i) &= \mathbf{a}(\omega_0 \frac{d_0}{c}\sin\theta_0)\frac{1}{N}\sum_{i=0}^{N-1}\mathbf{S}_0(\omega_i)\mathbf{a}^H(\omega_0 \frac{d_0}{c}\sin\theta_0) \\
&\quad + \mathbf{a}(\omega_0 \frac{d_0}{c}\sin\theta_1)\frac{1}{N}\sum_{i=0}^{N-1}\mathbf{S}_1(\omega_i)\mathbf{a}^H(\omega_0 \frac{d_0}{c}\sin\theta_1) + \sigma_\eta^2\mathbf{I}
\end{aligned} \tag{5.43}
$$

The above procedure for focusing may be extended to P sources; some of them may be correlated. While the idea of resampling is conceptually simple its implementation would require us to perform interpolation of the wavefield in between physical sensors. Fortunately, this is possible because in a homogeneous medium the wavefield is limited to a spatial frequency range, $u^2+v^2 \le \frac{\omega^2}{c^2}$ (see chapter 1, p. 14). In two dimensions, the spatial frequency range is $-\frac{\omega}{c} \le u \le \frac{\omega}{c}$; hence the wavefield is spatially bandlimited. This fact has been exploited in [21] for resampling.

The interpolation filter is a lowpass filter with its passband given by $-\frac{\omega}{c} \le u \le \frac{\omega}{c}$. Consider a ULA with sensor spacing equal to d_0 ($d_0 = \frac{\lambda}{2}$). The maximum temporal frequency will be $\omega_{\max} = \pi \frac{c}{d_0}$. The low pass filter is given by

$$h(m) = \frac{\sin \omega_{\max} \frac{(x-md_0)}{c}}{\omega_{\max} \frac{(x-md_0)}{c}}, \quad m = 0, \pm 1, \ldots, \pm\infty \tag{5.44}$$

where x denotes the point where interpolation is desired, for example, $x = m' d_k$ where $d_k = \frac{d_0 \omega_{\max}}{\omega_k}$.

5.2.3 Spatio Temporal Covariance Matrix (STCM): In chapter 2 we introduced the concept of extended direction vector (chapter 2, p. 129) and STCM using the extended direction vector and the source spectrum (2.67) which we reproduce here for convenience,

$$\mathbf{C}_{STCM} =$$

$$E\left\{\mathbf{f}_{stacked}(t)\mathbf{f}^H_{stacked}(t)\right\} = \frac{1}{2\pi}\int_{-\infty}^{\infty} \mathbf{h}(\omega,\varphi_0)\mathbf{h}^H(\omega,\varphi_0) S_{f_0}(\omega) d\omega \tag{2.67}$$

In this subsection we shall show how the STCM can be used for the direction of arrival estimation of a broadband source. For this it is necessary that the eigenstructure, in particular, the rank of STCM, will have to be ascertained. This has been done for a ULA in [23] and for a UCA in [24, 4]. We shall assume that the source spectrum is a smooth function and that it may be approximated by a piecewise constant function

$$S_{f_0}(\omega) \approx \sum_{l=-L}^{l=L} S_{0l}\, rect(\omega - \Delta\omega l) \qquad (5.45)$$

where

$$\begin{aligned} rect(\omega - \Delta\omega l) &= \frac{1}{\Delta\omega} \quad for \quad \Delta\omega(l - \frac{1}{2}) \le \omega \le \Delta\omega(l + \frac{1}{2}) \\ &= 0 \qquad otherwise \end{aligned}$$

and S_{0l} $(S_{0,l} = S_{0,-l})$ is the average spectrum in the l$^{\text{th}}$ frequency bin, $\Delta\omega l$. Using (5.45) in (2.67) we obtain

$$\mathbf{C}_{STCM} = \frac{1}{2\pi} \sum_{l=-L}^{l=L} S_{0l} \frac{1}{\Delta\omega} \int_{-\Delta\omega(l-\frac{1}{2})}^{\Delta\omega(l-\frac{1}{2})} \mathbf{h}(\omega,\varphi_0)\mathbf{h}^H(\omega,\varphi_0) d\omega \qquad (5.46)$$

where we have divided the frequency interval $\pm\pi$ into 2L+1 nonoverlapping frequency bins $(= \frac{2\pi}{\Delta\omega})$. Using the definition of the extended direction vector given in (2.67) in the integral in (5.46) we obtain the following result:

$$\frac{1}{2\pi\Delta\omega} \int_{-\Delta\omega(l-\frac{1}{2})}^{\Delta\omega(l-\frac{1}{2})} \mathbf{h}(\omega,\varphi_0)\mathbf{h}^H(\omega,\varphi_0) d\omega = \mathbf{g}_l \mathbf{Q} \mathbf{g}_l^H$$

where

$$\mathbf{g}_l = $$

$$diag\left\{ \begin{matrix} e^{-j\omega\tau_0}, e^{-j\omega\tau_1}, \ldots, e^{-j\omega\tau_{M-1}}; e^{-j\omega(\Delta t+\tau_0)}, e^{-j\omega(\Delta t+\tau_1)}, \ldots, \\ e^{-j\omega(\Delta t+\tau_{M-1})}; \ldots; e^{-j\omega((N-1)\Delta t+\tau_0)}, e^{-j\omega((N-1)\Delta t+\tau_1)}, \ldots, \\ e^{-j\omega((N-1)\Delta t+\tau_{M-1})} \end{matrix} \right\} \Bigg|_{\omega=\Delta\omega l}$$

and

$$[\mathbf{Q}]_{\alpha,\alpha'} = \operatorname{sinc}\left[((n-n')\Delta t + \tau_m - \tau_{m'}) \frac{\Delta\omega}{2} \right]$$

where $\alpha = m + n \times M$, $\alpha' = m' + n' \times M$, $n, n' = 0,1,\ldots,N-1$ and $m, m' = 0,1,\ldots,M-1$. Note that the time delays $(\tau_0, \tau_1, \ldots, \tau_{M-1})$ depend upon the array geometry and, of course, on the azimuth; for example, for a linear array, the time delays are $(0, \frac{d}{c}\sin\varphi, \ldots, (M-1)\frac{d}{c}\sin\varphi)$ and for a circular array the time delays are $(\delta\cos\varphi, \delta\cos(\frac{2\pi}{M}-\varphi), \ldots,$ $\delta\cos(\frac{2\pi}{M}(M-1)-\varphi))$ where $\delta = \frac{a}{c}$ and a is the radius of the circular array. Equation (5.46) may be expressed as

$$\mathbf{C}_{STCM} = \sum_{l=-L}^{l=L} S_{0l}\mathbf{g}_l \mathbf{Q} \mathbf{g}_l^H \tag{5.47}$$

The rank of $\mathbf{C}_{STCM}$ is determined by the rank of matrix $\mathbf{Q}$. It follows from the results in [11, 24] that 99.99% energy is contained in the first $\left[((N-1)\Delta t + \frac{2a}{c})\frac{\Delta\omega}{2\pi} + 1\right]$ eigenvalues of $\mathbf{Q}$ where [x] denotes the next integer greater than x. A comparison of the theoretical and numerically determined rank of $\mathbf{C}_{STCM}$ is given in fig. 5.5 for a circular array. For a linear array the corresponding number is given by $\left[((N-1)\Delta t + \frac{(M-1)d\cos\varphi}{c})\frac{\Delta\omega}{2\pi} + 1\right]$ [19]. Note that the dimension of the signal subspace is approximately equal to the time bandwidth product.

When the size of the observation space, that is, dimensions of $\mathbf{C}_{STCM}$, is larger than the rank of $\mathbf{C}_{STCM}$, $NM > \left[((N-1)\Delta t + \frac{2a}{c})\frac{\Delta\omega}{2\pi} + 1\right]$, there exists a null subspace, a subspace of the observation space, of dimension equal to

$$Dim\{\mathbf{v}_{null}\} = NM - \left[((N-1)\Delta t + \frac{2a}{c})\frac{\Delta\omega}{2\pi} + 1\right]$$

where $\mathbf{v}_{null}$ eigenvectors correspond to the insignificant eigenvalues. Note that the null subspace thus defined will not be an ideal null space with zero power; some residual power (<0.01%) will be present.

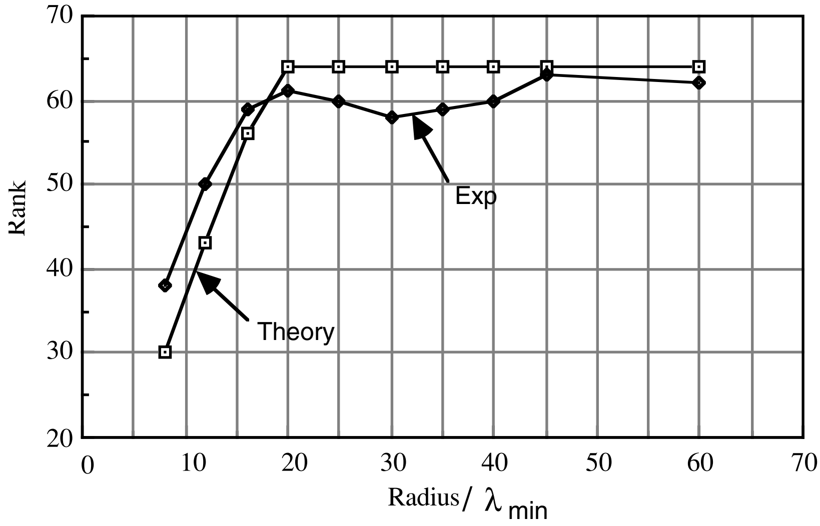

Figure 5.5: The effective rank of signal only STCM as a function of the radius of a circular array. The drop in the rank at radius $30\lambda_{\min}$ is due to a transition from smooth spectrum to line spectrum. We have considered a sixteen sensor equispaced circular array with other parameters N=4, B=0.8 (normalized bandwidth) and one source.(From [4]. © 1994, With permission from Elsevier Science)

Now, consider the following quadratic,

$$\begin{aligned}\mathbf{v}_i^H \mathbf{C}_{STCM} \mathbf{v}_i &= \frac{1}{2\pi}\int_{-\infty}^{\infty} \mathbf{v}_i^H \mathbf{h}(\omega,\varphi_0)\mathbf{h}^H(\omega,\varphi_0)\mathbf{v}_i S_{f_0}(\omega)d\omega \\ &= \frac{1}{2\pi}\int_{-\infty}^{\infty} \left|\mathbf{v}_i^H \mathbf{h}(\omega,\varphi_0)\right|^2 S_{f_0}(\omega)d\omega \approx 0\end{aligned} \tag{5.48}$$

Assume that $S_{f_0}(\omega) > 0$ over some frequency band. For (5.48) to hold good we must have in that frequency band

$$\left|\mathbf{v}_i^H \mathbf{h}(\omega,\varphi_0)\right|^2 \approx 0 \quad i \in null\, space \tag{5.49}$$

Equation (5.49) is the basic result used for estimation of φ_0. For the purpose of locating the null we can define a parametric spectrum as in narrowband MUSIC.

5.2.4 Number of Sources: We have so far assumed that the number of sources is known *a priori* or can be estimated from the knowledge of the significant and the repeated eigenvalues of the spectral matrix. The need for this information arises in the estimation of signal and noise subspaces. In time series analysis the equivalent problem is estimation of the number of sinusoids or estimation of the order of a time series model. A lot of effort has gone into this problem in time series analysis [25]. In this section we shall describe a test known as the sphericity test and its modern versions for estimating the number of repeated eigenvalues. Let P plane wavefronts be incident on an M sensor array. A covariance matrix of size $M \times M$ (M>P) has been computed using a finite number of N snapshots. Let $\hat{\lambda}_1 > \hat{\lambda}_2 > \hat{\lambda}_3 > ... > \hat{\lambda}_M$ be the eigenvalues of the estimated spectral matrix. We begin with the hypothesis that there are p wavefronts; then a subset of smaller eigenvalues, $\hat{\lambda}_{p+1} > \hat{\lambda}_{p+2} > ... > \hat{\lambda}_M$, is equal (or repeated). The null hypothis, that the smallest eigenvalues has a multiplicity of M-p, is tested starting at p=0 till the test fails. Mauchley [26] suggested a test known as the sphericity test to verify the equality of all eigenvalues of an estimated covariance matrix. Define a likelihood ratio statistic

$$\Gamma(\hat{\lambda}_{p+1}, \hat{\lambda}_{p+2}, ..., \hat{\lambda}_M) = \ln\left[\frac{\left(\frac{1}{M-p}\sum_{i=p+1}^{M}\hat{\lambda}_i\right)^{M-p}}{\prod_{i=p+1}^{M}\hat{\lambda}_i}\right]^N \tag{5.50a}$$

where N stands for number of snapshots. The log likelihood ratio is then compared with a threshold γ. Whenever

$$\Gamma(\hat{\lambda}_{p+1}, \hat{\lambda}_{p+2}, ..., \hat{\lambda}_M) > \gamma$$

the test is said to have failed. Modified forms of the sphericity tests have been suggested in References [27, 28].

The choice of γ is subjective. Alternate approaches which do not require a subjective judgment have been proposed [29]. The number of wavefronts is given by that value of p in the range 0 to $M-1$ where, either

$$\Gamma(\hat{\lambda}_{p+1}, \hat{\lambda}_{p+2}, ..., \hat{\lambda}_M) + p(2M-p) \tag{5.50b}$$

or

$$\Gamma(\hat{\lambda}_{p+1},\hat{\lambda}_{p+2},\ldots,\hat{\lambda}_M)+\frac{p}{2}(2M-p)\ln N \tag{5.50c}$$

is minimum. The first form is known as Akaike information criterion (AIC) and the second form is known as minimum description length (MDL). The expression consists of two parts; the first part is the log likelihood ratio which decreases monotonically and the second part is a penalty term which increases monotonically as p increases from 0 to $M-1$. The penalty term is equal to free adjusted parameters. The log likelihood ratio plot around p=P undergoes a rapid change of slope, which is responsible for the occurrence of a minimum at p=P. This is demonstrated in fig. 5.6.

The performance of AIC and MDL criteria has been studied in the context of detection of plane waves incident on a linear array in [30]. They define a probability of error as

$$prob.of\ error = prob\left(p_{\min} < P \middle| H_P\right) + prob\left(p_{\min} > P \middle| H_P\right)$$

where $p_{\min}$ stands for the position of the minimum of (5.50) and H_P denotes the hypothesis that the true number of signal sources is P. The probability of error for the MDL criterion monotonically goes to zero for a large number of snapshots or high snr. In contrast, the probability of error for the AIC criterion tends to a small finite value. However, for a small number of snapshots or low snr the performance of AIC is better than that of MDL.

§5.3 **Coded Signals**:

In communication a message bearing signal is specifically designed to carry maximum information with minimum degradation. In analog communication, amplitude modulated and frequency modulated signals are often used while in digital communication each pulse representing a bit is modulated with a sine wave (frequency shift keying) or with a pseudorandom sequence (spread spectrum). From the signal processing point, as these signals belong to a class of cyclostationary processes whose covariance function is periodic, but the background noise is simple ordinary stochastic process, these differences have been exploited in array processing for the direction arrival estimation. Sometimes, it is necessary to localize an active source for improved communication as in dense wireless telephone user environment. Here we would like to emphasize how a specially coded signal leads us to newer approaches to localization. We shall demonstrate with three different types of coded signals, namely, (i) multitone signal where the tones are spaced at prescribed frequency intervals but with random phases, (ii) binary phase shift keying (BPSK) signal and (iii) cyclostationary signals.

5.3.1 Multitone Signal: Consider a circular boundary array (see chapter 2) of M equispaced, omnidirectional, wideband sensors (fig. 5.7) with a target which is

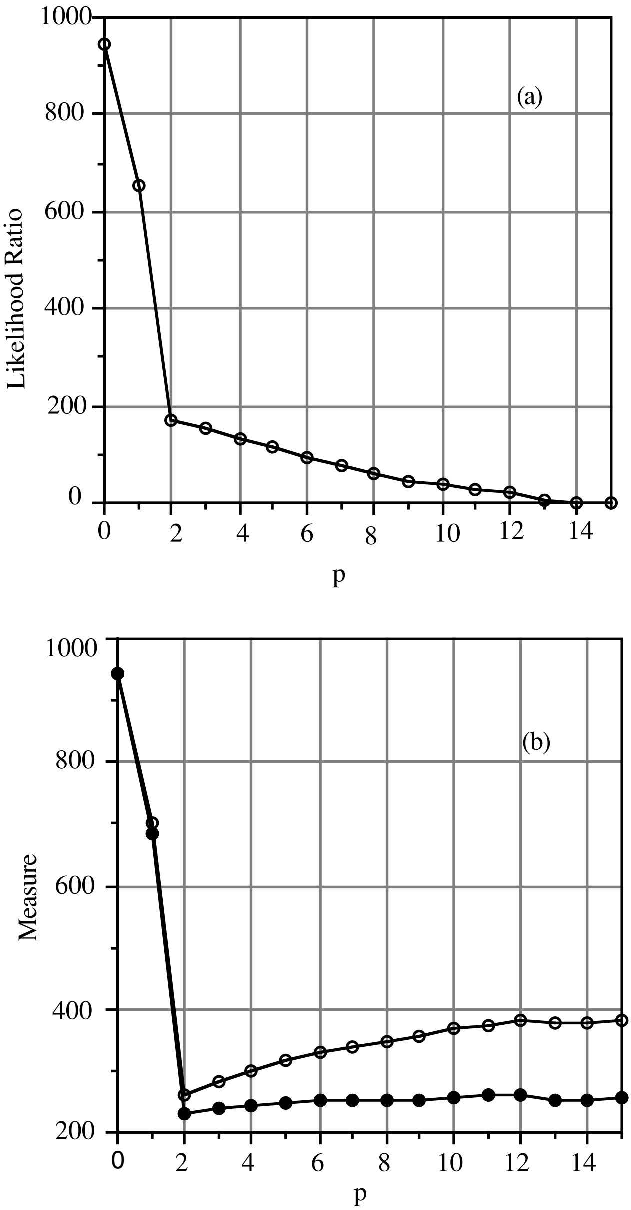

Figure 5.6: (a) Log likelihood ratio as a function of p, number of assumed wavefronts, (b) AIC (filled circles) and MDL (empty circles) as a function of p. Note the minimum at p=2. 20 frequency snapshots. 16 sensor ULA with $\lambda/2$ spacing. Two uncorrelated wavefronts are incident at angles 24^{o} and 32^{o}. snr=10 db per source.

surrounded by the array. A source is assumed at a point with polar coordinates (r,φ) and it radiates a signal which is a sum of harmonically related random sinusoids,

$$f(t)=\sum_{k=0}^{Q-1}\alpha_k e^{-j(\omega_0+k\Delta\omega)t} \tag{5.51}$$

where α_k is the complex amplitude of kth sinusoid. The output of the ith sensor is given by $f_i(t)=f(t+\Delta\tau_i)+\eta_i(t)$, where $\Delta\tau_i$ is time delay at the ith sensor with respect to a fictitious sensor at the center of the array. Each sensor output is tapped at N time instants and arranged in a vector form,

$$\mathbf{f}_i=col\{f_i(0),f_i(1),\ldots f_i(N-1)\}$$

The output data vector of the ith sensor may be written in a compact form shown below:

$$\mathbf{f}_i=a(r_i)\mathbf{H}\mathbf{A}_i\varepsilon+\eta_\text{i} \qquad 5.52)$$

where

$$\begin{aligned}
&\mathbf{H}=[\mathbf{h}_0,\mathbf{h}_1,\ldots\mathbf{h}_{Q-1}]\\
&\mathbf{h}_k=col\{1,e^{j\omega_k},\ldots e^{j(N-1)\omega_k}\}\\
&\omega_\text{k}=\omega_0+\text{k}\Delta\omega\\
&\mathbf{A}_i=diag\{e^{j\omega_0\Delta\tau_i},e^{j\omega_1\Delta\tau_i},\ldots e^{j\omega_{Q-1}\Delta\tau_i}\}\\
&\varepsilon=\text{col}[\alpha_0,\alpha_1,\ldots\alpha_{Q-1}]
\end{aligned}$$

Next, we shall stack up all data vectors into one large vector **F** of dimension MNx1. It may be expressed as

$$\mathbf{F}=\mathbf{TDE}+\eta \tag{5.53}$$

where

$\mathbf{T}=diag\{\mathbf{H},\mathbf{H},\ldots\mathbf{H}\}$,(NMxMQ),
$\mathbf{D}=diag\{a(r_0)\mathbf{A}_0,a(r_1)\mathbf{A}_1,\ldots a(r_{M-1})\mathbf{A}_{M-1}\}$, (MQxMQ) and
$\mathbf{E}=[\varepsilon^\text{T},\varepsilon^\text{T},\varepsilon^\text{T},\ldots]^\text{T}$, (MQx1)

The covariance matrix (STCM) of **F** is given by

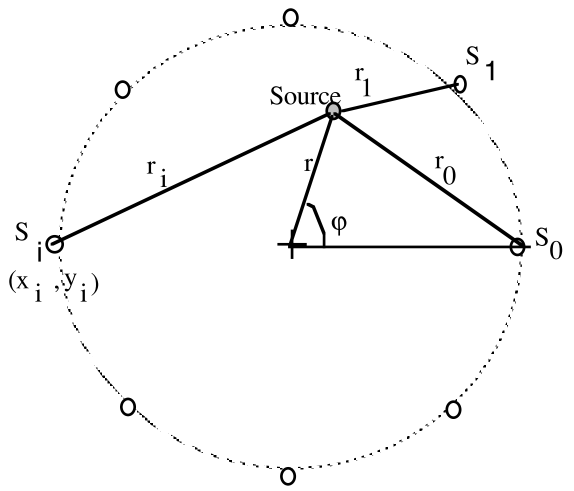

Figure 5.7: A circular array of sensors and a source inside the circle. The range (r) and azimuth (φ) of the source and all time delays are measured with respect to the center of the array as shown.

$$\mathbf{c}_f = \mathbf{T}\mathbf{D}\Gamma_0\mathbf{D}^H\mathbf{T}^H + \sigma_\eta^2\mathbf{I}$$

where $\Gamma_0 = E\left\{\mathbf{E}\mathbf{E}^H\right\} = \mathbf{1}\otimes\Gamma$ where $\mathbf{1}$ is a square matrix of size MxM whose elements are all equal to 1, $\Gamma = diag\{\gamma_0, \gamma_1, \ldots \gamma_{Q-1}\}$ and $\gamma_0, \gamma_1, \ldots \gamma_{Q-1}$ are powers of the random sinusoids. Symbol $\otimes$ stands for Kronecker product. We will assume hereafter that the noise variance σ_η^2 is known or has been estimated from the array output when there is no signal transmission or by averaging the noise eigenvalues of the covariance matrix and that it has been subtracted from the covariance matrix.

Let us consider the structure of the mth column of the STCM. By straightforward multiplication it can be shown that the mth column of the covariance matrix is given by

$$\mathbf{c}_m = \left[\mathbf{c}_m^{0^T}, \mathbf{c}_m^{1^T}, \ldots, \mathbf{c}_m^{Q-1^T}\right]^T \tag{5.54}$$

where $\mathbf{c}_m^i = a(r_i)a(r_0)\mathbf{H}\mathbf{A}_i\Gamma\mathbf{A}_o^H\mathbf{H}^H\mathbf{u}_m$ and $\mathbf{u}_m$ is a Mx1 vector consisting of all zeros except at m$^{\text{th}}$ location where there is one. Note $\mathbf{A}_i\Gamma\mathbf{A}_0^H$ is a diagonal matrix given by

$$\mathbf{A}_i\Gamma\mathbf{A}_0^H = diag\{\gamma_0 e^{j\omega_0\mu_i}, \gamma_1 e^{j\omega_1\mu_i}, \ldots \gamma_{Q-1} e^{j\omega_{Q-1}\mu_i}\} \tag{5.55}$$

where $\mu_i = \Delta\tau_i - \Delta\tau_0$. Further, we note that

$$\mathbf{H}^H\mathbf{u}_m = \mathrm{col}\{e^{-jm\omega_0}, e^{-jm\omega_1}, \ldots e^{-jm\omega_{Q-1}}\} \tag{5.56}$$

Using (5.55) and (5.56) in (5.54) we obtain

$$\begin{aligned}
&\mathbf{C}_m^i = a(r_i)a(r_0)\times \\
&\mathbf{H}col\left\{\gamma_0 e^{j\omega_0(\mu_i - m)}, \gamma_1 e^{j\omega_1(\mu_i - m)}, \ldots \gamma_{Q-1} e^{j\omega_{Q-1}(\mu_i - m)}\right\}
\end{aligned} \tag{5.57}$$

Multiply on both sides of (5.57) by $\mathbf{H}^\# = (\mathbf{H}^H\mathbf{H})^{-1}\mathbf{H}^H$, the pseudo-inverse of **H,** and obtain

$$\mathbf{H}^\#\mathbf{C}_m^i = a(r_i)a(r_0)col\left\{\gamma_0 e^{j\omega_0(\mu_i - m)}, \gamma_1 e^{j\omega_1(\mu_i - m)}, \ldots \gamma_{Q-1} e^{j\omega_{Q-1}(\mu_i - m)}\right\}$$

We now define a matrix **D** whose columns are $\mathbf{H}^\#\mathbf{C}_m^i$, i=0, 1, 2, ... M-1,

$$\begin{aligned}
\mathbf{D} &= \left\{\mathbf{H}^\#\mathbf{C}_m^0, \mathbf{H}^\#\mathbf{C}_m^1, \ldots \mathbf{H}^\#\mathbf{C}_m^{M-1}\right\} \\
&= a^2(r_0)diag\left\{\gamma_0 e^{-j\omega_0 m}, \gamma_1 e^{-j\omega_1 m}, \ldots \gamma_{Q-1} e^{-j\omega_{Q-1} m}\right\}
\end{aligned} \tag{5.58}$$

where

$$\mathbf{G} = \begin{bmatrix}
1, b_1 e^{j\omega_0\mu_1}, \ \ldots b_{M-1} e^{j\omega_0\mu_{M-1}} \\
1, b_1 e^{j\omega_1\mu_1}, \ \ldots b_{M-1} e^{j\omega_1\mu_{M-1}} \\
\ldots \\
\ldots \\
1, b_1 e^{j\omega_{Q-1}\mu_1}, \ldots b_{M-1} e^{j\omega_{Q-1}\mu_{M-1}}
\end{bmatrix}$$

Source #1		Source #2	
Range	Azimuth	Range	Azimuth
24.99 (25.00)	50.01 (50.00)	30.00 (30.00)	50.02 (50.00)
89.99 (90.00)	90.00 (90.00)	70.01 (70.00)	-90.00 (-90.00)
9.99 (10.00)	29.99 (30.00)	50.02 (50.00)	150.02 (150.00)
50.01 (50.1)	-60.00 (-60.00)	49.99 (50.00)	-60.00 (-60.00)

Table 5.4: Localization of two sources by a circular (boundary) array of 8 sensors. snr=10 dB. The STCM was averaged over one hundred independent estimates. The wave speed was assumed as 1500 meters/sec. The numbers inside brackets represent the true values (range in meters and azimuth in degrees).

and $b_i = \dfrac{a(r_i)}{a(r_0)}$, i=0,1,...,M-1. Since the location information is present in $\mu_0, \mu_1, \ldots \mu_{M-1}$, our aim naturally is to estimate these from the columns of **G**. Each column may be considered as a complex sinusoid whose frequency can be estimated, provided $|\Delta\omega\mu_i| \le \pi$. For a boundary array, specifically a circular array, this limitation can be overcome. In chapter 2 we have given an algorithm to estimate time delays or the location of the source from the phase estimates.

As a numerical example we have considered two sources each emitting eight random tones. The frequencies emitted by the first source are (0, 200, 400, 600, 800, 1000, 1200, 1400 Hz) and those by the second are (1600, 1800, 2000, 2200, 2400, 2600, 2800, 3000 Hz). An eight sensor UCA of radius 100 meters surrounds both sources. Sixteen delayed snapshots (taps) were used making the size of STCM as 128x128. The results are displayed in table 5.4.

5.3.2 BPSK Signal: Binary phase shift keying signal consists of square pulses of fixed width with amplitude given by a Bernoulli random variable, an outcome of a coin tossing experiment where head equals +1 and tail equals -1. A typical BPSK sequence is shown in fig. 5.8. The analytic representation of BPSK signal is given by

$$c_0(t) = \sum_{n=0}^{L-1} c_{0,n} h_{T_c}(t - nT_c) \qquad (5.59a)$$

where $c_{0,n}$, n=0,1,...,L-1 are Bernoulli random variables and $h_{T_c}(t)$ is a

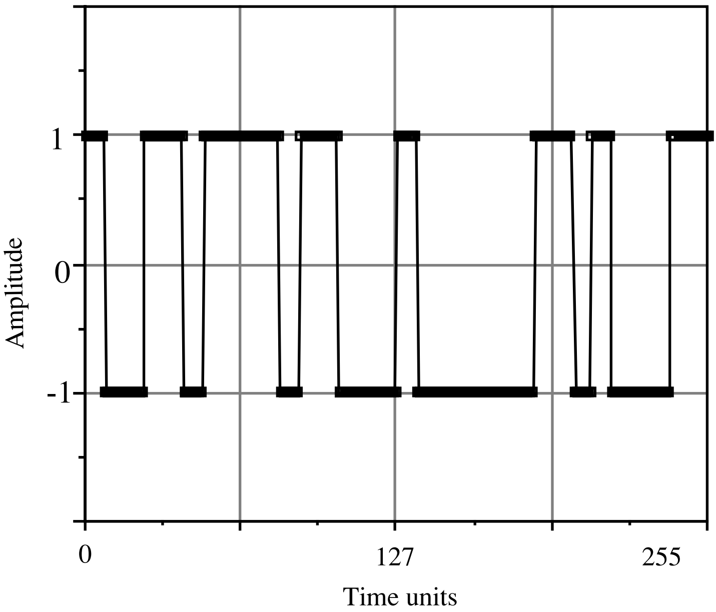

Figure 5.8: BPSK waveform. A train of rectangular pulses with amplitude alternating between +1 and -1.

rectangular function of width T_c. One of the most useful properties of a BPSK sequence is its narrow autocorrelation function with sidelobes whose variance is less than the inverse of the sequence length. We can easily generate many uncorrelated BPSK sequences. BPSK sequences have beenused for time delay measurement [31], digital communication [32], and mobile communication [33] where it is of interest to exploit the spatial diversity for the purpose of increasing the capacity. Here we shall briefly show how the azimuth of a source emitting a known BPSK signal may be estimated.

The signal model considered here is as in [34]. There are Q uncorrelated sources emitting data bits which are encoded with a user specific random sequence, a BPSK sequence, for example.

$$x_m(t) = \sum_{k=0}^{Q} p_k a_m(\theta_k) \sum_l b_{k,l} c_k(t - lT_s - \tau_k) + \eta_m(t) \qquad (5.59b)$$
$$m = 0,1,2,\ldots M-1$$

where

$a_m(\theta_k)$: response of mth sensor to a signal coming from kth user

p_k: signal amplitude of k^{th} user
$b_{k,l}$: data stream from k^{th} user
$c_k(t)$: random code of k^{th} user
T_S: bit duration
τ_k: delay of a signal from k^{th} user
$\eta_m(t)$: Noise at m^{th} sensor
Q : number of users

There are two different approaches to DOA estimation with BPSK coded signal. In the first approach the usual covariance matrix is computed and in the second approach, due to the fact that the code used by the user of interest is known, the received signal is first cross-correlated with that code. The output of the cross-correlator is then used to compute the covariance matrix. Both approaches yield similar results; though in the second approach the interference from the users of no interest is reduced by a factor proportional to the code length.

Precorrelation Covariance Matrix: The outputs of the sensor array, after removing the carrier, are arranged in a vector form,

$$\mathbf{f}(t) = \sum_{k=0}^{Q} p_k \mathbf{a}(\theta_k) \sum_{l} b_{k,l} c_k(t - lT_s - \tau_k) + \eta(t) \tag{5.60a}$$

where $\mathbf{f}(t)$, $\mathbf{a}(\theta_k)$, and $\eta(t)$ are Mx1 vectors. The precorrelation covariance matrix is given by

$$\mathbf{c}_f = E\{\mathbf{f}(t)\mathbf{f}^H(t)\} \tag{5.60b}$$

Using (5.60a) in (5.60b) we obtain

$$\mathbf{c}_f = \left\{ \begin{bmatrix} \sigma_\eta^2 \mathbf{I} + \sum_{k=0}^{Q} \sum_{k'=0}^{Q} p_k p_{k'} \mathbf{a}(\theta_k) \mathbf{a}(\theta_{k'}) \\ \left\{ \sum_{l} \sum_{l'} b_{k,l} c_k(t - lT_s - \tau_k) b_{k',l'} c_{k'}(t - l'T_s - \tau_{k'}) \right\} \end{bmatrix} \right\} \tag{5.60c}$$

We shall assume that the data bits coming from different users are independent and codes assigned to different users are uncorrelated. As a result, (5.60c) reduces to

$$\mathbf{c}_f = \left\{ \sum_{k=0}^{Q} p_k^2 \mathbf{a}(\theta_k) \mathbf{a}(\theta_k) \left\{ \sum_l b_{k,l}^2 c_k^2 (t - lT_s - \tau_k) \right\} \right\} + \sigma_\eta^2 \mathbf{I}$$

But the quantity inside the inner curly brackets is always equal to 1; hence we obtain

$$\mathbf{c}_f = \left\{ \sum_{k=0}^{Q} p_k^2 \mathbf{a}(\theta_k) \mathbf{a}(\theta_k) \right\} + \sigma_\eta^2 \mathbf{I}$$

which may be expressed in a standard form (4.12b) as

$$\begin{aligned} \mathbf{c}_f &= \left[\mathbf{a}(\theta_0), \mathbf{a}(\theta_1), \ldots, \mathbf{a}(\theta_{Q-1}) \right] diag\left\{ p_0^2, p_1^2, \ldots, p_{Q-1}^2 \right\} \\ &\quad \left[\mathbf{a}(\theta_0), \mathbf{a}(\theta_1), \ldots, \mathbf{a}(\theta_{Q-1}) \right]^H + \sigma_\eta^2 \mathbf{I} \\ &= \mathbf{A}\, diag\left\{ p_0^2, p_1^2, \ldots, p_{Q-1}^2 \right\} \mathbf{A}^H + \sigma_\eta^2 \mathbf{I} \end{aligned} \tag{5.60d}$$

Postcorrelation Covariance Matrix: The outputs of the antenna array, after removing the carrier, are correlated with the desired user code assuming synchronization has been achieved. The postcorrelation array signal vector corresponding to the l^{th} bit is given by

$$\mathbf{g}_0(l) = \frac{1}{T_s} \int_{lT_s}^{(l+1)T_s} \mathbf{f}(t) c_0 (t - lT_s) dt \tag{5.61}$$

where $\mathbf{f}(t)$ stands for array signal vector without carrier. Using the signal model given by (5.60a), eq. (5.61) may be written as

$$\begin{aligned} &\mathbf{g}_0(l) = \\ &\frac{1}{T_s} p_0 \mathbf{a}(\theta_0) \int_{lT_s}^{(l+1)T_s} \Big[\sum_{j=-\infty}^{\infty} b_{0j} c_0 (t - jT_s) \Big] c_0 (t - lT_s) dt \\ &+ \frac{1}{T_s} \sum_{k=1}^{Q-1} p_k \mathbf{a}(\theta_k) \int_{lT_s}^{(l+1)T_s} \Big[\sum_{-\infty}^{\infty} b_{kj} c_k (t - jT_s + \tau_k) \Big] c_0 (t - lT_s) dt \\ &+ \frac{1}{T_s} \int_{lT_s}^{(l+1)T_s} \eta(t) c_0 (t - lT_s) dt \end{aligned} \tag{5.62}$$

where we have set $\tau_0 = 0$. In (5.62) the first term, equal to b_{0k}, is the signal term. The second term represents the interference. It is evaluated as follows: The integral is split into two parts, lT_s *to* $lT_s + \tau_k$, and $lT_s + \tau_k$ *to* $(l+1)T_s$. After a change of variable it reduces to

$$\frac{1}{T_s}\sum_{k=1}^{Q-1} p_k \mathbf{a}(\theta_k)\left[b_{kl-1}\int_0^{\tau_k} c_k(t - T_s - \tau_k)c_0(t)dt + b_{kl}\int_0^{\tau_k} c_k(t-\tau_k)c_0(t)dt\right]$$

$$= \mathbf{b}_l^1 + \mathbf{b}_l^2 \tag{5.63}$$

Finally, the noise term reduces to

$$\eta_1 = \frac{1}{T_s}\int_0^{T_s} \eta(t + lT_s)c_0(t)dt$$

The postcorrelation covariance matrix of the array signal is given by

$$\begin{aligned}\mathbf{C}_{g_0 g_0} &= E\left\{\mathbf{g}_0(l)\mathbf{g}_0^H(l)\right\} \\ &= p_0^2\mathbf{a}(\theta_0)\mathbf{a}^H(\theta_0) + E\{\mathbf{b}_l^1\mathbf{b}_l^{1^H}\} + E\{\mathbf{b}_l^2\mathbf{b}_l^{2^H}\} + E\{\eta_l\eta_l^H\}\end{aligned} \tag{5.64a}$$

All cross terms vanish. First, we shall evaluate $E\{\mathbf{b}_l^1\mathbf{b}_l^{1^H}\}$.

$$E\{\mathbf{b}_l^1\mathbf{b}_l^{1^H}\} = \frac{1}{T_s^2}\sum_{k=1}^{Q} p_k^2\mathbf{a}(\theta_k)\mathbf{a}(\theta_k)^H\rho_1 \tag{5.64b}$$

where

$$\rho_1 = E\left\{\left[\int_0^{\tau_k} c_k(t + T_s - \tau_k)c_0(t)dt\right]^2\right\}$$

and the sources are assumed to be uncorrelated. Using the representation of BPSK signal (5.59a) we obtain

$$\rho_1 =$$

$$E\left\{\left[\int_0^{\tau_k}\sum_{m_0}^{L-1}\sum_{m_k}^{L-1} c_{0,m_0}c_{k,m_k}h_{T_c}(t - m_0T_c)h_{T_c}(t + T_s - m_kT_c - \tau_k)dt\right]^2\right\}$$

which, on account of the fact that c_{0,m_0} and c_{k,m_k} are uncorrelated random variables, reduces to

$$\rho_1 = \frac{1}{T_s}\int_0^{T_s}\sum_{m_0}^{L-1}\sum_{m_k}^{L-1}\left[\int_0^{\tau_k} \begin{matrix} h_{T_c}(t-m_0T_c) \\ h_{T_c}(t+T_s-m_kT_c-\tau_k)dt \end{matrix}\right]^2 d\tau_k \tag{5.65a}$$

where τ_k, the arrival time of the signal from the kth user, is assumed to be uniformly distributed over 0 to T_s, the symbol duration. The integral over τ_k may be expressed as a sum over L integrals, one for each chip. When h_{T_c} is a rectangular function the integral with respect to τ_k in (5.65a) can be evaluated in a closed form. After some algebraic manipulations we obtain

$$\rho_1 = \frac{L^2}{3T_s}T_c^3 \tag{5.65b}$$

Substituting (5.65b) in (5.64b) we obtain

$$E\{\mathbf{b}_l^1\mathbf{b}_l^{1^H}\} = \frac{1}{3L}\sum_{k=1}^{Q} p_k^2\mathbf{a}(\theta_k)\mathbf{a}(\theta_k)^H \tag{5.66a}$$

Evaluation of $E\{\mathbf{b}_l^2\mathbf{b}_l^{2^H}\}$ proceeds on the same lines as above. In fact the result is identical, that is,

$$E\{\mathbf{b}_l^2\mathbf{b}_l^{2^H}\} = \frac{1}{3L}\sum_{k=1}^{Q} p_k^2\mathbf{a}(\theta_k)\mathbf{a}(\theta_k)^H = E\{\mathbf{b}_l^1\mathbf{b}_l^{1^H}\} \tag{5.66b}$$

Finally, we shall evaluate the noise term in (5.62).

$$\begin{aligned} E\{\eta_l\eta_l^{\mathrm{H}}\} &= \frac{1}{T_s^2}E\left\{\int_0^{T_s}\int_0^{T_s}\eta(t_1+lT_s)\eta^{\mathrm{H}}(t_2+lT_s)c_0(t_1)c_0(t_2)dt_1dt_2\right\} \\ &= \frac{1}{T_s^2}\sum_{m_1=0}^{L-1}\int_0^{T_c}\int_0^{T_c} \begin{matrix} E\left\{\eta(t_1+lT_c)\eta^{\mathrm{H}}(t_2+lT_c)\right\} \\ h_{T_c}(t_1-m_1T_c)h_{T_c}(t_2-m_1T_c)dt_1dt_2 \end{matrix} \\ &= \frac{\sigma_\eta^2}{L}\mathbf{I} \end{aligned} \tag{5.67}$$

where we assumed that the noise is spatially uncorrelated but temporally correlated over the chip width T_c. Using equations (5.65b), (5.66) and (5.67) in (5.64) the postcorrelation covariance matrix may be expressed as

$$\mathbf{c}_{g_0 g_0} = p_0^2 \mathbf{a}(\theta_0)\mathbf{a}^H(\theta_0) + \frac{2}{3L}\sum_{k=1}^{Q} p_k^2 \mathbf{a}(\theta_k)\mathbf{a}^H(\theta_k) + \frac{\sigma_\eta^2}{L}\mathbf{I} \tag{5.68}$$

which may be expressed in a standard form (4.12b)

$$\begin{aligned}\mathbf{c}_{g_0 g_0} &= \left[\mathbf{a}(\theta_0),\mathbf{a}(\theta_1),\ldots,\mathbf{a}(\theta_{Q-1})\right] diag\left\{p_0^2,\frac{2}{3L}p_1^2,\ldots,\frac{2}{3L}p_{Q-1}^2\right\} \\ &\quad \left[\mathbf{a}(\theta_0),\mathbf{a}(\theta_1),\ldots,\mathbf{a}(\theta_{Q-1})\right]^H + \frac{\sigma_\eta^2}{L}\mathbf{I} \\ &= \mathbf{A}diag\left\{p_0^2,\frac{2}{3L}p_1^2,\ldots,\frac{2}{3L}p_{Q-1}^2\right\}\mathbf{A}^H + \frac{\sigma_\eta^2}{L}\mathbf{I}\end{aligned} \tag{5.69}$$

The directions of arrival (DOA) may be estimated following the subspace approach described earlier in §5.1 and §5.2.

5.3.3 Cyclostationary Signals: A signal defined in (5.58) and other similar communication signals possess an important property, namely, its temporal covariance function is periodic. This is a result of transmission of symbols at a fixed rate and also due to the use of a periodic carrier. Indeed the periodicity in the covariance function of the signal, also known as cyclic frequency α, is equal to lf_b where l is an integer and f_b is baud rate, that is, the number of symbols transmitted per second. The baud rate is a unique property associated with each source and it is not affected by propagation. Since the baud rate of a signal of interest (SOI) is known a priori and it is different from that of the other interfering signals, it is possible to distinguish the SOI from the interference and the system noise whose covariance function is known to be aperiodic. In this section we shall describe how a subspace method, i.e., MUSIC, may be devised by exploiting the property of cyclostationarity. The background information on cyclostationary process will not be covered here as such material is already available in a book [35] and in a popular exposition [36]. However, we shall introduce enough material that is essential for the understanding of its application to DOA estimation.

Let $\mathbf{f}(t) = \left\{f_0(t), f_0(t-\frac{d}{c}\sin\theta_0),\ldots,f_0(t-(M-1)\frac{d}{c}\sin\theta_0)\right\}$

be the output of a M sensor array on which a cyclostationary signal $f_0(t)$ is incident with an angle of incidence θ_0. We define frequency shifted versions of $\mathbf{f}(t)$

$$\begin{aligned}\mathbf{f}_+(t) &= \mathbf{f}(t)e^{j\pi\alpha t}\\ \mathbf{f}\_(t) &= \mathbf{f}(t)e^{-j\pi\alpha t}\end{aligned} \tag{5.70}$$

and cyclic covariance matrix

$$\begin{aligned}\mathbf{c}_f^\alpha(\tau) &= \frac{1}{T}\sum_{t=-\frac{T}{2}}^{\frac{T}{2}} E\left\{\mathbf{f}\_(t+\frac{\tau}{2})\mathbf{f}_+^H(t-\frac{\tau}{2})\right\}\\ &= \frac{1}{T}\sum_{t=-\frac{T}{2}}^{\frac{T}{2}} E\left\{\mathbf{f}(t+\frac{\tau}{2})\mathbf{f}^H(t-\frac{\tau}{2})\right\}e^{-j2\pi\alpha t}\\ &\quad T\to\infty\end{aligned}$$

Let us show how to evaluate the (k,l)th element of the matrix $\mathbf{c}_f^\alpha(\tau)$.

$$\begin{aligned}&\left[\mathbf{c}_f^\alpha(\tau)\right]_{kl}\\ &= \frac{1}{T}\sum_{t=-\frac{T}{2}}^{\frac{T}{2}} E\left\{f_0^*(t+k\frac{d}{c}\sin\theta_0-\frac{\tau}{2})f_0(t+l\frac{d}{c}\sin\theta_0+\frac{\tau}{2})e^{-j2\pi\alpha t}\right\}\\ &\qquad T\to\infty\\ &= c_{f_0}^\alpha(\tau+(k-l)\frac{d}{c}\sin\theta_0)e^{j\pi\alpha(k+l)\frac{d}{c}\sin\theta_0}\end{aligned} \tag{5.71a}$$

When a source is narrowband with center frequency ω_c so that following approximation holds good, $f_0(t+\tau)\approx f_0(t)e^{j\omega_c\tau}$ (see (4.15b)), the (k,l)th element of the matrix $\mathbf{c}_f^\alpha(\tau)$ may be approximated as $\left[\mathbf{c}_f^\alpha(\tau)\right]_{kl}\approx c_{f_0}^\alpha(\tau)e^{j\omega_c(k-l)\frac{d}{c}\sin\theta_0}e^{j\pi\alpha(k+l)\frac{d}{c}\sin\theta_0}$, which may be further approximated as $\left[\mathbf{c}_f^{\alpha}(\tau)\right]_{kl} \approx c_{f_0}^{\alpha}(\tau)e^{j\omega_c(k-l)\frac{d}{c}\sin\theta_0}$ for $\omega_c >> 2\pi\alpha$. Using the narrowband approximation and the assumption $\omega_c >> 2\pi\alpha$ we can express the cyclic covariance matrix as

$$\mathbf{c}_f^{\alpha}(\tau) \approx \mathbf{a}_0\mathbf{a}_0^H c_{f_0}^{\alpha}(\tau) \tag{5.71b}$$

The above relation is quite similar to (4.12b), which was the starting point in the subspace algorithm, for example, in MUSIC. Naturally, based on (5.71b), a subspace algorithm known as Cyclic MUSIC has been proposed in [37]. Although, in deriving (5.71b) we have assumed a single source, it holds good even in the presence of multiple signals with *different* cyclic frequencies and any type of stationary noise.

Let us consider the diagonal terms of the cyclic covariance matrix. From (5.71a) the diagonal terms, k=l, are given by

$$\left[\mathbf{c}_f^{\alpha}(\tau)\right]_{k=l} = c_{f_0}^{\alpha}(\tau)e^{j2\pi\alpha l\frac{d}{c}\sin\theta_0} \tag{5.72a}$$

which we shall express in a matrix form. Let

$$\tilde{\mathbf{c}}_f^{\alpha}(\tau) = col\left\{\left[\mathbf{c}_f^{\alpha}(\tau)\right]_{k=l=0},\left[\mathbf{c}_f^{\alpha}(\tau)\right]_{k=l=1},\ldots,\left[\mathbf{c}_f^{\alpha}(\tau)\right]_{k=l=M-1}\right\}$$
$$\mathbf{a}(\alpha,\theta_0) = col\left\{1, e^{j2\pi\alpha\frac{d}{c}\sin\theta_0},\ldots,e^{j2\pi\alpha(M-1)\frac{d}{c}\sin\theta_0}\right\}$$

and using these vectors, (5.72a) may be written as

$$\tilde{\mathbf{c}}_f^{\alpha}(\tau) = c_{f_0}^{\alpha}(\tau)\mathbf{a}(\alpha,\theta_0) \tag{5.72b}$$

and for P uncorrelated sources, but with the same cyclic frequency, we obtain

$$\tilde{\mathbf{c}}_f^{\alpha}(\tau) = \left\{\mathbf{a}(\alpha,\theta_0),\mathbf{a}(\alpha,\theta_1),\ldots,\mathbf{a}(\alpha,\theta_{P-1})\right\}\begin{bmatrix} c_{f_0}^{\alpha}(\tau) \\ \ldots \\ c_{f_{P-1}}^{\alpha}(\tau)\end{bmatrix} \tag{5.72c}$$

Note that in deriving (5.72) we have not used the narrowband approximation which was earlier used in deriving (5.71b). The computer simulation results reported in [38] showed improved results obtained by using (5.72c) over (5.71b) except when the bandwidth is only a tiny fraction (<0.05) of the carrier frequency. In (5.72b) or (5.72c) the noise term is absent as it is not a cyclostationary process. This is a very important feature of any system using the cyclostationary signals. Whether the noise is correlated or white its cyclostationary autocorrelation function at any cyclic frequency vanishes. Another important feature of great signficance is that the condition of two sources being mutually cyclically uncorrelated is weaker than the condition of mutually uncorrelated. Two cyclostationary signals f(t) and g(t) are said to be uncorrelated if their cross-cyclic covariance function defined as

$$c_{fg}^{\alpha}(\tau) = \frac{1}{T} \sum_{t=-\frac{T}{2}}^{\frac{T}{2}} E\left\{ f^{*}(t-\frac{\tau}{2}) g(t+\frac{\tau}{2}) \right\} e^{-j2\pi\alpha t} \qquad (5.73)$$

$$T \to \infty$$

vanishes for all τ and α is equal to the cyclic frequency either of f(t) or g(t). To demonstrate this property let us consider $f(t) = s(t)\cos(\omega_1 t + \theta_1)$ and $g(t) = s(t)\cos(\omega_2 t + \theta_2)$ and substituting in (5.73) we obtain

$$c_{fg}^{\alpha}(\tau) =$$

$$c_s(\tau) \frac{1}{2T} \sum_{t=-\frac{T}{2}}^{\frac{T}{2}} \begin{bmatrix} \cos((\omega_1+\omega_2)t - (\omega_1-\omega_2)\frac{\tau}{2} + \theta_1 + \theta_2) \\ +\cos((\omega_1-\omega_2)t - (\omega_1+\omega_2)\frac{\tau}{2} + \theta_1 - \theta_2) \end{bmatrix} e^{-j2\pi\alpha t}$$

$$T \to \infty$$

which becomes zero except when $2\pi\alpha = \pm(\omega_1 + \omega_2)$ or $= \pm(\omega_1 - \omega_2)$. Thus, two sources transmitting the same message but with different carriers become cyclically uncorrelated. Generalizing the above result, P sources transmitting even the same message but with different carrier frequencies may become *cyclically uncorrelated*. Further, we notice that even when the carrier frequencies are the same, the sources can become cyclically uncorrelated unless we choose $2\pi\alpha = \pm 2\omega_1$ or 0. As a result, it is possible through an appropriate choice of α to selectively cancel all signals of no interest. As a numerical example, we computed the cyclic cross-correlation function between two sources radiating the same stochastic signal with different carrier frequencies. In fig. 5.9a the cyclic cross-correlation function is shown as a function of the cyclic frequency. The carrier frequencies are 0.15 Hz and 0.20 Hz. (The Nyquist frequency is 0.5 Hz and 1024 time samples were used.)

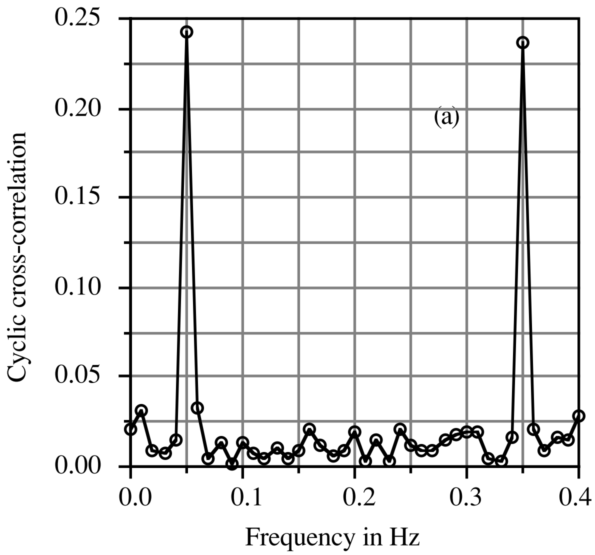

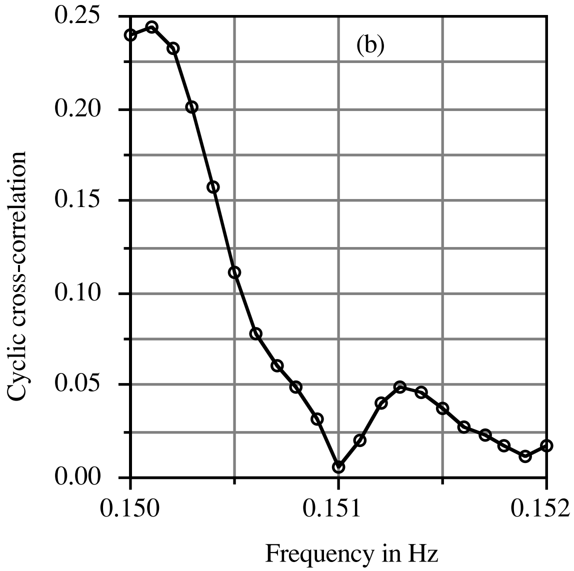

Figure 5.9: Cyclic cross-correlation function at zero lag as a function of (a) cyclic frequency and (b) carrier frequency in Hz.

Note the peaks at the sum and difference frequencies. In fig. 5.9a the cyclic cross-correlation function is shown as a function of the carrier frequency of the second source.

§5.4 **Array Calibration**:

Throughout we have implicitly assumed that all sensors are ideal, that is, they are omnidirectional point sensors with constant response. Further, the shape of the array is fully known. If we are dealing with a ULA we assume that all sensors are on a perfectly straight line and sensors are equispaced. Any deviations from the assumptions can cause considerable loss of performance, particularly in the use of subspace methods [39]. One way out of this limitation is to actually measure the properties of the array, including its shape, and use this information in the design of the processor. Often this requires a source whose location is known. The properties of the array can be measured, a process known as array calibration. We shall describe two types of calibrations. In the first instance we shall give a method of computing the amplitude and the phase variations. Next we shall describe a method for the shape estimation, which is vital in the use of flexible arrays.

5.4.1 Amplitude and Phase Variation of a Sensor:

From (2.17e) the direction vector may be expressed as a product of two components

$$\mathbf{a}(\theta_0) = \alpha(\theta_0)\phi(\theta_0)$$

where

$$\alpha(\theta_0) = diag\{\alpha_0(\theta_0), \alpha_1(\theta_0), \ldots \alpha_{M-1}(\theta_0)\}$$

$$\phi(\theta_0) = \mathrm{col}\{1, e^{-j\omega\frac{d}{c}\sin\theta_0}, e^{-j\omega\frac{2d}{c}\sin\theta_0} \ldots e^{-j\omega\frac{(M-1)d}{c}\sin\theta_0}\}$$

The purpose of array calibration is to estimate $\alpha(\theta_0)$ from actual array observations. We preclude the possibility of direct in-situ measurement of sensor sensitivity (hardware calibration). Recall the relation we had derived between the direction vectors and eigenvectors of $\mathbf{v}_s\mathbf{v}_s^H$ (5.6d). Consider a single source whose direction of arrival is known. For single source (5.6d) may be expressed as

$$\alpha(\theta_0)\phi(\theta_0) = \mathbf{v}_s\mathbf{v}_s^H\alpha(\theta_0)\phi(\theta_0) \tag{5.74}$$

Clearly $\alpha(\theta_0)\phi(\theta_0)$ is an eigenvector of $\mathbf{v}_s\mathbf{v}_s^H$ and the corresponding eigenvalue is 1. Since the direction of arrival of the source is known we can compute $\phi(\theta_0)$ and demodulate the eigenvector. We can thus estimate $\alpha(\theta_0)$

but for a complex constant. Assume that $\alpha(\theta_0)$ is independent of θ_0. We shall express (5.74) in a different form. Note that

$$\alpha\phi(\theta_0) = diag\{\alpha_0, \alpha_1 e^{-j\omega\frac{d}{c}\sin\theta_0}, \ldots \alpha_{M-1} e^{-j\omega\frac{(M-1)d}{c}\sin\theta_0}\}$$
$$= diag\{1, e^{-j\omega\frac{d}{c}\sin\theta_0}, \ldots e^{-j\omega\frac{(M-1)d}{c}\sin\theta_0}\} col\{\alpha_0, \ldots \alpha_{M-1}\}$$
$$= \phi_d(\theta_0)\alpha_c$$

Using the above result in (5.74) we obtain

$$\alpha_c = \phi_d^H(\theta_0)\mathbf{v}_s \mathbf{v}_s^H \phi_d(\theta_0)\alpha_c \tag{5.75a}$$

When there are P sources with known DOAs, $\theta_p, p = 0,1,\ldots,P-1$ (5.75a) may be expressed as $\alpha_c = \mathbf{Q}\alpha_c$ where

$$\mathbf{Q} = \sum_{p=0}^{P-1} \phi_d^H(\theta_p)\mathbf{v}_s \mathbf{v}_s^H \phi_d(\theta_p) \tag{5.75b}$$

and α_c is the eigenvector of $\mathbf{Q}$ corresponding to its largest eigenvalue equal to P [40].

5.4.2 Shape Estimation: In any practical towed array system used in sonar or seismic exploration the position of sensors is continuously monitored. Additionally, it is also possible to estimate the shape from the array output. Here from the point of array signal processing our natural interest is in the second approach. Consider a ULA which has been deformed either on account of towing or ocean currents. Assume that we have a known source radiating a narrowband signal and the background noise is spatially uncorrelated. We have shown in (5.4) the eigenvector of the spatial covariance matrix corresponding to the largest eigenvalue is proportional to the direction vector. In fact, the relation is given by $\mathbf{v}_0 = \frac{1}{\sqrt{M}}\mathbf{a}_0$. For deformed array the direction vector may be obtained from (2.34c)

$$\mathbf{a}(\theta_0, \varphi_0) = col\left\{\begin{matrix} 1, e^{-j\omega_c \frac{d}{c}[\gamma_1 \sin\theta_0 \sin\varphi_0 + \varepsilon_1 \sin\theta_0 \cos\varphi_0 + \xi_1 \sin\theta_0]}, \ldots, \\ e^{-j\omega_c \frac{d}{c}[\gamma_{M-1} \sin\theta_0 \sin\varphi_0 + \varepsilon_{M-1} \sin\theta_0 \cos\varphi_0 + \xi_{M-1} \sin\theta_0]} \end{matrix}\right\} \tag{5.76}$$

Therefore, we can relate the eigenvector to the direction vector

$$\mathbf{v}_0 = \frac{1}{\sqrt{M}} col \left\{ \begin{matrix} 1, e^{-j\omega_c \frac{d}{c}[\gamma_1 \sin\theta_0 \sin\varphi_0 + \varepsilon_1 \sin\theta_0 \cos\varphi_0 + \xi_1 \sin\theta_0]}, \ldots, \\ e^{-j\omega_c \frac{d}{c}[\gamma_{M-1} \sin\theta_0 \sin\varphi_0 + \varepsilon_{M-1} \sin\theta_0 \cos\varphi_0 + \xi_{M-1} \sin\theta_0]} \end{matrix} \right\} \tag{5.77a}$$

Note that since the source is known, its azimuth and elevation are known a priori. The unknowns are $\gamma_m, \varepsilon_m, m = 0,1,\ldots,M-1$. (Note $\xi_m, m = 0,1,\ldots,M-1$ are dependent on γ_m, ε_m.) To solve for a pair of unknowns we would need one more source, say, with different azimuth and elevation, (θ_1, φ_1). Once again the largest eigenvector may be related to the direction vector of the second source.

$$\mathbf{v}_1 = \frac{1}{\sqrt{M}} col \left\{ \begin{matrix} 1, e^{-j\omega_c \frac{d}{c}[\gamma_1 \sin\theta_1 \sin\varphi_1 + \varepsilon_1 \sin\theta_1 \cos\varphi_1 + \xi_1 \sin\theta_1]}, \ldots, \\ e^{-j\omega_c \frac{d}{c}[\gamma_{M-1} \sin\theta_1 \sin\varphi_1 + \varepsilon_{M-1} \sin\theta_1 \cos\varphi_1 + \xi_{M-1} \sin\theta_1]} \end{matrix} \right\} \tag{5.77b}$$

We shall, for the sake of simplicity, assume that the deformed array is in the x-y plane and also place the calibrating source in the x-y plane. Then, a single source is enough for estimation of γ_m and ε_m which now take a form

$$\begin{aligned} \gamma_m &= \sum_{i=0}^{m} \cos\alpha_i, \quad m = 0,1,\ldots,M-1 \\ \varepsilon_m &= \sum_{i=0}^{m} \sin\alpha_i, \quad m = 0,1,\ldots,M-1 \end{aligned} \tag{5.78}$$

Using (5.78) in (5.77b) we obtain the following basic result

$$\begin{aligned} &\frac{\lambda_c}{2\pi}\left[\angle\{\mathbf{v}_0\}_m - \angle\{\mathbf{v}_0\}_{m-1}\right] + \lambda_c n = \\ &d\cos\alpha_m \cos\varphi_0 + d\sin\alpha_m \sin\varphi_0 = \Delta x_m \cos\varphi_0 + \Delta y_m \sin\varphi_0 \end{aligned} \tag{5.79}$$

where n is an unknown integer and Δx_m and Δy_m are x,y coordinates of mth sensor relative to m-1st sensor. The ambiguity, arising out of the unknown integer, may be resolved through geometrical considerations. Note that the mth sensor must be on a circle of radius d centered at

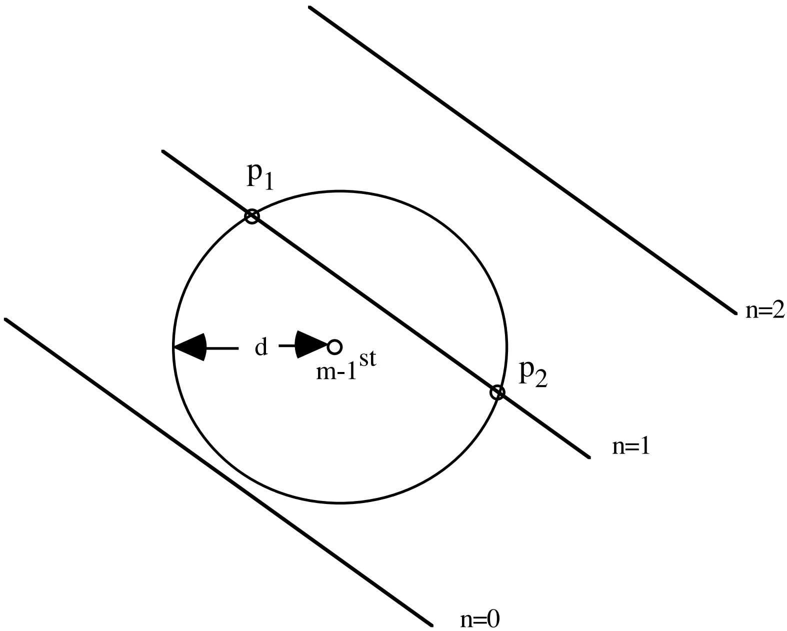

Figure 5.10 The ambiguity in (5.77) is resolved by requiring that the line it represents must intersect the circle of radius d drawn at m-1st sensor. There are two intersection points. The sensor may be at any one of the two intersections.

m-1st sensor. Further the position of the sensor must satisfy (5.79), which, incidentally, is an equation of a straight line [41]. For illustration let the line corresponding to n=1 intersect the circle at two points p_1 and p_2 (see fig. 5.10). The sensor can either be at p_1 or p_2. This ambiguity is resolved by choosing a point which results in minimum array distortion [42].

§5.5 **Source in Bounded Space**:

When a source is in a bounded space a sensor array will receive signals reflected from the boundaries enclosing the space, for example, radar returns from a low flying object [43], an acoustic source in shallow water [44], a speaker in a room [45]. In all these cases the reflections are strongly correlated with the direct signal and come from a set of predictable directions. The complexity of the multipath structure increases with the increasing number of reflecting surfaces, as illustrated in fig. 5.11. We shall in this section briefly consider two simple cases involving one reflecting surface (a low flying object) and two reflecting surfaces (an acoustic source in shallow water) shown in fig. 5.11a & b.

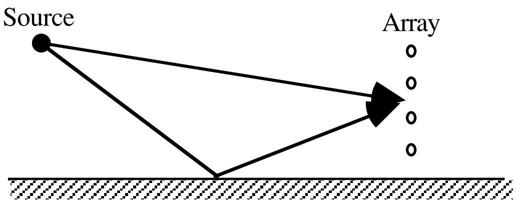

(a)

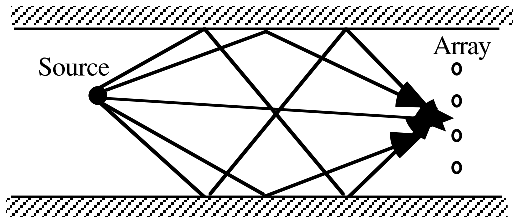

(b)

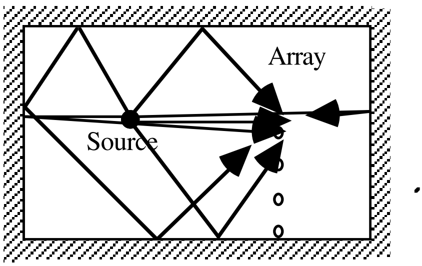

(c)

Figure 5.11: Three examples of multipath structure with increasing complexity. Assuming the boundaries are well defined we can predict the multipaths given the source and array locations.

5.5.1 <u>Single Reflecting Surface</u>: Assume that the source emits a stationary stochastic signal. A vertical sensor array is used to receive the signal radiated by the source. The array output in frequency domain may be written in terms of the radiated signal as follows:

$$d\mathbf{F}(\omega) = \mathbf{a}_0 dF_0(\omega) + w_1 e^{-j\omega\tau_1}\mathbf{a}_1 dF_0(\omega) + d\mathrm{N}(\omega)$$
$$= [\mathbf{a}_0, \mathbf{a}_1][1, w_1 e^{-j\omega\tau_1}]^T dF_0(\omega) + d\mathrm{N}(\omega) \tag{5.80}$$

where $dF_0(\omega)$ is the differential of the generalized Fourier transform of stochastic signal emitted by the source, $d\mathrm{N}(\omega)$ is the differential of the generalized Fourier transform of the background noise presumed to be spatially and temporally white and $\mathbf{a}_0$, and $\mathbf{a}_1$ are the direction vectors of direct and reflected signals, respectively,

$$\mathbf{a}_0 = col\left\{1, e^{-j\omega\frac{d}{c}\sin\theta_0}, \ldots, e^{-j\omega(M-1)\frac{d}{c}\sin\theta_0}\right\}$$

$$\mathbf{a}_1 = col\left\{1, e^{-j\omega\frac{d}{c}\sin\theta_1}, \ldots, e^{-j\omega(M-1)\frac{d}{c}\sin\theta_1}\right\}$$

τ_1 is the delay of the reflected signal relative to the direct arrival and w_1 stands for reflection coefficient. The spectral matrix of the array output is easily derived from (5.80)

$$\mathbf{S}_f(\omega) = [\mathbf{a}_0, \mathbf{a}_1][1, w_1 e^{-j\omega\tau_1}]^T [1, w_1 e^{-j\omega\tau_1}][\mathbf{a}_0, \mathbf{a}_1]^H S_0(\omega) + \sigma_\eta^2 \mathbf{I} \tag{5.81}$$

Define $\tilde{\mathbf{a}} = [\mathbf{a}_0, \mathbf{a}_1][1, w_1 e^{-j\omega\tau_1}]^T = \mathbf{a}_0 + w_1 e^{-j\omega\tau_1}\mathbf{a}_1$ and rewrite (5.81) as

$$\mathbf{S}_f(\omega) = \tilde{\mathbf{a}} S_0(\omega) \tilde{\mathbf{a}}^H + \sigma_\eta^2 \mathbf{I} \tag{5.82}$$

Note that (5.82) is of the same form as (4.12b). Naturally, it is possible to derive a subspace algorithm to estimate the parameters, θ_0 and θ_1; alternatively, range and height of the source above the reflecting surface, in terms of which θ_0 and θ_1, can be expressed. The Music spectrum is now a function of two parameters, range and height, instead of frequency as in the conventional Music spectrum. For this reason it may be worthwhile to call it a parametric spectrum. A numerical example of parametric spectrum for a source situated above a reflecting surface and an eight sensor vertical ULA is given in fig. 5.12. The peak of the parametric spectrum is correctly located but this good result has been achieved because we have used the exact value of the reflection coefficients. Even a small error, on the order of 1%, appear to completely alter

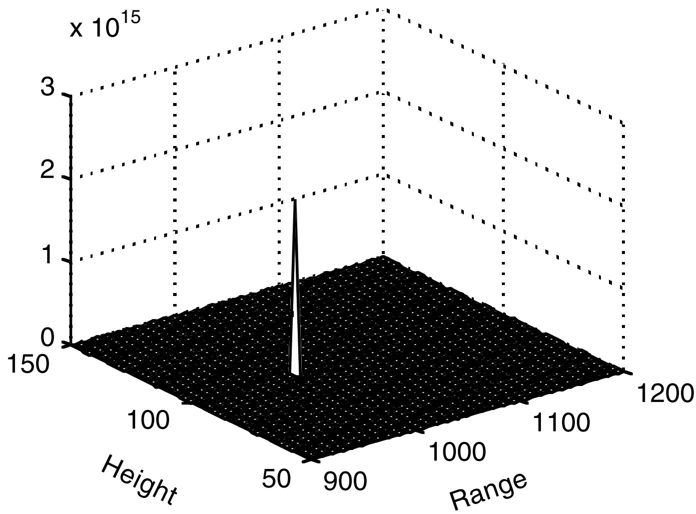

Figure 5.12: Parametric spectrum for a source situated above a reflecting surface (100λ) and 1000λ away from an eight element vertical ULA. The array center is at 16λ above the reflecting surface.

the picture; in particular, the range estimation becomes very difficult.

5.5.2 Two Reflecting Surfaces: To keep the analysis reasonably simple we shall confine ourselves to two parallel reflecting surfaces and a vertical ULA. A broadband signal is assumed, as simple frequency averaging seems to yield good results (see fig. 5.13). Consider a uniform channel of depth H meters where a vertical array of equispaced (spacing $d_0<\lambda/2$) sensors is located at depth z_R (depth is measured from the surface of the channel to the top sensor of the array) and a source of radiation at a depth z_s and is horizontally separated by a distance R_0 from the array. We have noted in chapter 1 (page 26) that depending upon the range and the channel characteristics the array would be able to see a certain number of significant images, say P. The waveform received from P images at m^{th} sensor (m=0 is the top sensor) is given by

$$f_m(t)=\sum_{p=0}^{P-1}\frac{\alpha_p}{R_p}f_0(t-\tau_{pm})+\eta_m(t) \tag{5.83}$$

where $f_0(t)$ is the signal emitted by the source, presumed to be a stationary stochastic process, τ_{pm} is time delay from p^{th} image to m^{th} sensor, R_p is the

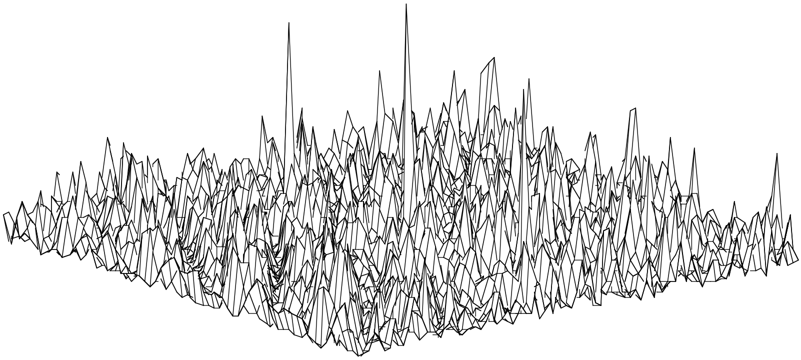

(a)

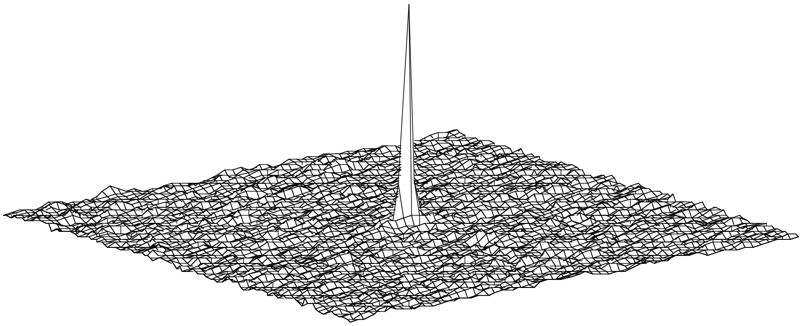

(b)

Figure 5.13: (a) Parametric spectrum at 1600 Hz is shown as a function of range and depth. A broadband acoustic source is assumed at 2000m (range) and 25m (depth) in a channel of depth 100m. Twenty frequency snapshots were used to compute the spectral matrix. Next, the parametric spectra computed at 50 frequencies, equispaced in the band 1000Hz to 2000Hz, were averaged. The averaged spectrum is shown in (b). (From [47]. © 1999, With permission from Elsevier Science)

distance to the pth image and α_p is the reflection coefficient for the ray arriving from the pth image. $\eta_m(t)$ is noise received by the mth sensor. It is easy to show that

$$\tau_{pm} = \tau_p + (m-1)\frac{d}{c}\sin\theta_p \tag{5.84}$$

where τ_p is travel time from pth image to the top sensor and θ_p is azimuth angle (with respect to the horizontal plane) of the wave vector from pth image and c is sound speed in sea water. This angle can be computed from the geometry of the image structure as shown in fig.1.14. Using the spectral representation of the stationary stochastic process (5.83) may be written in the frequency domain as

$$dF_m(\omega) = \sum_{p=0}^{P-1} w_p dF_0(\omega) e^{j(m-1)2\pi \frac{d}{\lambda}\sin\theta_p} + d\mathrm{N}_m(\omega) \qquad (5.85)$$

where $w_p = \dfrac{\alpha_p}{R_p} e^{j\omega\tau_p}$ [44]. Let us express (5.85) in a compact matrix notation by defining

$$\mathbf{A} = \begin{bmatrix} 1 & \cdots & 1 \\ e^{j\omega \frac{d}{c}\sin\theta_0} & \cdots & e^{j\omega \frac{d}{c}\sin\theta_{P-1}} \\ & \cdots & \\ e^{j\omega \frac{d}{c}(M-1)\sin\theta_0} & \cdots & e^{j\omega \frac{d}{c}(M-1)\sin\theta_{P-1}} \end{bmatrix}$$

and $\mathbf{w} = col[w_0, w_1, \ldots, w_{P-1}]$. Equation (5.85) may be written in a matrix form,

$$d\mathbf{F}(\omega) = \mathbf{A}\mathbf{w}dF_0(\omega) + d\mathrm{N}(\omega) \qquad (5.86)$$

The spectral matrix is obtained from (5.86) by squaring and averaging

$$\mathbf{S}_f(\omega) = \mathbf{A}\mathbf{w}\mathbf{w}^H\mathbf{A}^H S_{f_0}(\omega) + \sigma_\eta^2\mathbf{I} \qquad (5.87)$$

where $S_{f_0}(\omega)$ (scalar) is the spectrum of the source radiation, and σ_η^2 is the variance of the background noise. Define a vector $\tilde{\mathbf{A}} = \mathbf{A}\mathbf{w}$ and rewrite (5.87) as

$$\mathbf{S}_f(\omega) = \tilde{\mathbf{A}} S_{f_0}(\omega) \tilde{\mathbf{A}}^H + \sigma_\eta^2\mathbf{I} \qquad (5.88)$$

Note that the structure of spectral matrix in (5.88) is the same as in (4.12b). This enables us to develop a subspace algorithm to estimate unknown parameters, range and depth of the source (also azimuth, if a horizontal array is used) [44].

Source localization in a bounded space is prone to errors in the assumed model as well as the estimation errors due to finite available data. The geometry of the channel needs` to be specified with an accuracy of a fraction of wavelength and the wavespeed must be known accurately. In practice these requirements are often difficult to satisfy. However, it is possible, at the cost of increased array length, to achieve good results when the channel is only partially known [46]. Good results have also been obtained with limited data but using a broadband signal as demonstrated in fig. 5.13 [47].

§5.6 **Exercises:**

1. The line represented by (5.79) intersects the circle at two points p_1 and p_2 (see fig. 5.10). Let two adjacent sensors be on the x-axis. Show that one of the points will be at the intersection of the x-axis and circle. Where will be the second point?

2. In chapter 4 (4.13a) it was shown that $\mathbf{A}^H\mathbf{Q}=\mathbf{0}$ where $\mathbf{Q}$ was defined in terms of partitions of the spectral matrix. Is $\mathbf{Q}$ itself the noise subspace? Remember that in obtaining $\mathbf{Q}$ no eigendecomposition was required.

3. Show that, taking into account the variation in the sensitivity of the sensors, equation (5.72b) takes the form

$$\tilde{\mathbf{c}}_f^\alpha(\tau)=c_f^\alpha(\tau)\alpha_2(\theta_0)\mathbf{a}(\alpha,\theta_0)$$

where

$$\alpha_2(\theta_0)=diag\{\left|\alpha_0(\theta_0)\right|^2,\left|\alpha_1(\theta_0)\right|^2,\ldots,\left|\alpha_{M-1}(\theta_0)\right|^2\}.$$

Interestingly, phase variations themselves do not affect the relation given in (5.71b).

4. How would you cancel the interference coming from the users of no interest in equations (5.60d) and (5.69)? Can you also cancel the term due to the noise?

5. In subsection 5.1.2 we have shown how to restore the rank of a rank deficient spectral matrix by smoothing the spectral matrices of subarrays. Show that this can also be achieved by smoothing of the signal subspace eigenvectors of the spectral matrix of the full array. This approach is suggested in [48] but on a covariance matrix.

6. Let **J** be an exchange matrix which collects all odd and even elements of a vector; for example, a 4x4 exchange matrix is

$$\mathbf{J}=\begin{bmatrix}1,0,0,0\\0,0,1,0\\0,1,0,0\\0,0,0,1\end{bmatrix}$$

Consider a ULA with M sensors and P uncorrelated wavefronts that are incident on the array. Let $\mathbf{v}_s$ be a matrix whose columns are the signal eigenvectors of the array spectral matrix. Show that $\mathbf{J}\mathbf{v}_s=\begin{bmatrix}\mathbf{A}\\\mathbf{A}\boldsymbol{\Gamma}\end{bmatrix}\mathbf{G}^{-1}$ where matrices $\mathbf{A}$ $(\frac{M}{2}\times P)$ and $\mathbf{G}$ $(P\times P)$ are as defined in (5.6c) and the $\Gamma\,(P\times P)$ is as defined in (2.57). This result provides an alternate approach to the ESPRIT algorithm described in §5.1. It can be used to extend the concept of subspace rotation to multiple subarrays as described in [49].

References

1. R. O. Schmidt, Multiple emitter location and signal parameter estimation, in Proc. of RADC Spectral Estimation Workshop, Griffiths AFB, New York, pp. 243-258, Reprinted in IEEE Trans. AP-34, pp. 276-280, 1986.
2. G. Bienvenu and L. Kopp, Principe de la goniometri passive adaptive, Proc. Colloque, CRESTI, Nice (France), pp. 106/1-10, 1979.
3. V. F. Pisarenko, The retrieval of harmonics from covariance function, Geophy. J. R. Astron. Soc., vol. 33, pp. 347-366, 1973.
4. C. U. Padmini and P. S. Naidu, Circular array and estimation of direction of arrival of a broadband source, Signal Proc., vol. 37, pp. 243-254, 1994.
5. A. B. Gershman and V. T. Ermolaev, Electronics Letters, vol. 28, pp. 1114-1115, 1992.
6. S. U. Pillai, *Array Signal Processing*, Springer-Verlag, New York, 1989.
7. A. B. Gershman and V. T. Ermolaev, Optimal subarray size for spatial smoothing, IEEE SP Letters, vol.2, pp. 28-30, 1995.
8. A. J. Barabell, Improving the resolution performance of eigenstructure based direction finding algorithm, IEEE Proc ICASSP, pp. 336-339, 1983.
9. B. D. Rao, Performance analysis of root Music, IEEE Trans., ASSP-37, pp. 1939-1049, 1989.
10. R. Roy, A. Paulraj, and T. Kailath, Direction of arrival estimation by subspace rotation method - ESPRIT, IEEE. Proc ICASSP, Tokyo, pp. 2495-2498, 1986.
11. D. Slepian and H. D. Pollack, and H. J. Landau, Prolate spheroidal wave function, Fourier analysis and uncertainty, Bell Systems Tech Jour., vol. 40, pp. 43-84, 1961.

12. U. Reddy, B. Egart, and T. Kailath, Least squares type algorithm for adaptive implementation of Pisarenko's harmonic retrieval method, IEEE Trans. ASSP-30, pp. 339-405, 1982.
13. P. Yang and M. Kaveh, Adaptive eigensubspace algorithm for direction or frequency estimation and tracking, IEEE Trans, ASSP-36, pp. 241-251, 1988.
14. J. Karhunen, Adaptive algorithms for estimation of eigenvectors of correlation type matrices, IEEE, Proc. ICASSP-84, pp. 14.6.1-4, 1984.
15. G. Stewart, *Introduction to Matrix Computations*, Academic Press, New York, 1973.
16. H. Wang and M. Kaveh, Coherent signal subspace processing for the detection and estimation of multiple wideband sources, IEEE, ASSP-30, pp. 823-831, 1985.
17. H. Wang and M Kaveh, Focussing matrices for coherent signal subspace processing, IEEE ASSP-36, pp. 1272-1281, 1988.
18. J. Krolick and D. N. Swinger, Focussed wideband array processing via spatial sampling, IEEE, ASSP-38, pp. 356-360, 1990.
19. K. M. Buckly and L. Griffiths, Broadband signal subspace spatial spectrum (BASS-ALE) estimation, IEEE ASSP-36, pp. 953-964, 1988.
20. D. N. Swinger and J. Krolik, Source location bias in the coherently focused high resolution broadband beamformation, IEEE ASSP-37, pp. 143-144, 1989.
21. J. Krolik and D. Swingler, Multiple broadband source location using steered covariance matrices, IEEE Trans. ASSP-37, pp. 1481-1494, 1989.
22. S. Valae and P. Kabal, Wideband array processing using a two sided correlation transformation, IEEE Trans SP-43, pp. 160-172, 1995.
23. K. M. Buckley and L. Griffiths, Eigenstructure based broadband source localization, IEEE, ICASSP-86, pp. 1867-1872, 1986.
24. C. Usha Padmini, Wideband source localization, ME dissertation, ECE Dept, IISc, Bangalore, India, 1991.
25. P. S. Naidu, *Modern Spectrum Analysis of Time Series*, CRC Press, Boca Raton,FL.,1996.26. J. W. Mauchley, Significance test for sphericity of a normal n-variate distribution, Ann. Math. Stat., vol.11. pp. 204-209, 1940.
27. W. S. Ligget, Jr., Passive sonar: fitting models to multiple time series, in Signal Processing: Proc. NATO ASI Signal Processing, J. W. R. Griffiths and P.L. Stocklin, Eds., Academic, New York, pp. 327-345, 1973.
28. D. B. Williams and D. H. Johnson, Using the sphericity test for source detection with narrow band passive array, IEEE Trans., ASSP-38, pp. 2008-2014, 1990.
29. M. Wax and T. Kailath, Detection of signals by information theoretic criteria, IEEE Trans., ASSP-33, pp. 387-392, 1985.
30. Qi-Tu Zhang, Kon Max Wong, P. C. Yip, and J. P. Reilly, Statistical analysis of the performance of information theoretic criteria in the detection of the number of signals in array processing, IEEE Trans., ASSP-39, pp. 1557-1567,1989.

31. J. P. Henrioux and G. Jourdain, Use of large bandwidth-duration binary phase shift keying signals for bearing measurements in active sonar classification, JASA, vol. 97, pp. 1737-1746, 1995.
32. R. L. Pickholz, D. L. Schilling, and L. B. Milstein, Theory of spread spectrum communications-A Tutorial, IEEE Trans COM-30, pp. 855-884, 1982.
33. R. L. Pickholz, L. B. Milstein, and D. L. Schilling, Spread spectrum for mobile communications, IEEE Trans.Vehicular Technology, vol. 40, pp. 313-322, 1991.
34. A. F. Naguib, A. Paulraj, and T. Kailath, Capacity improvement with base station antenna array in cellular CDMA, IEEE Trans.,vol. 43, pp. 691-698, 1994.
35. W. A. Gardner, *Introduction to Random Processes with Applicarion to Signals and Systems*, New York, MacMillan, 1985.
36. W. A Gardner, Exploitation of spectral redundancy in cyclostationarity signals, IEEE., Signal Proc. Mag., pp. 14-36, April 1991.
37. S. V. Schell, R. A. Calabretta, W. A. Gardner and B. G. Agee, Cyclic MUSIC algorithm for signal selective direction finding, Proc. ICASSP89, vol. 4, pp. 2278-2281, 1989.
38. G. Xu and T. Kailath, Direction of arrival estimation via exploitation of cyclostationarity- A combination of temporal and spatial processing, IEEE Trans., SP-40, pp. 1775-1786, 1992.
39.R. T. Compton, Pointing accuracy and dynamic range in steered beam adaptive array, IEEE Trans., AES-16, pp. 280-287, 1980.
40. V. C. Soon, L. Tong, Y. F. Huang, and R. Liu, A subspace method for estimating sensor gains and phases, IEEE Trans., SP-42, pp. 973-976, 1994.
41. J. J. Smith, Y. H. Leung, and A. Cantoni, The partitioned eigenvector method for towed array shape estimation, IEEE Trans SP-44, pp. 2273-2283, 1996.
42. D. A. Gray, W. O. Wolfe and J. L. Riley, An eigenvector method for estimating the positions of the elements of an array of receivers, Proc. ASSPA 89, Signal Processing theories, implementation, and applications, R. F. Barrett (Ed.), Adelaide Australia, pp. 391-393, 1989.
43. S. B. Kesler, J. Kesler and G. Levita, Resolution of coherent target in the near field of an array antenna, IEEE, Proc. ICASSP-86, pp. 1937-1940, 1986.
44. P. S. Naidu, A new method of acoustic source localization in shallow sea. Proc. Institute of Acoustics, vol. 18, part 5, pp. 39-48, 1996.
45. H. F. Silverman, Some analysis of microphone arrays for speech data acquisition, IEEE Trans., ASSP-35, pp. 1699-1712, 1987.
46. P. S. Naidu and T. Ganesan, Source localization in a partially known shallow water channel, Journ Acoust Soc of Am, vol. 98, pp. 2554-2559, 1995.
47. P. S. Naidu and H. Uday Shankar, Broadband source localization in shallow water, Signal Processing, vol.72, pp. 107-116, 1999.

48. S. S. Reddi and A.B. Gershman, An alternative approach to coherent source location proble, IEEE Trans. SP-59, pp. 221-233, 1997.
49. A. L. Swindlehurst, B. Ottersten, R. Roy, and T. Kailath, Multiple invariance ESPRIT, IEEE Trans. SP-40, pp. 867-881, 1992.
50. A. Papoulis, *Probability, Random Variables and Stochastic Processes*, Third edition, McGraw-Hill Book Co., New York, 1991.